Annu. Rev. Earth Planet. Sci. 2000. 28:391–417

SEISMIC IMAGING OF MANTLE PLUMES

Henri-Claude Nataf
Observatoire des Sciences de l'Univers de Grenoble, Grenoble Cedex 9, France; BP 53, 38041; e-mail: nataf@ujf-grenoble.fr

Key Words mantle plume, hotspot, seismic tomography, mantle convection

■ **Abstract** The mantle plume hypothesis was proposed thirty years ago by Jason Morgan to explain hotspot volcanoes such as Hawaii. A thermal diapir (or plume) rises from the thermal boundary layer at the base of the mantle and produces a chain of volcanoes as a plate moves on top of it.

The idea is very attractive, but direct evidence for actual plumes is weak, and many questions remain unanswered. With the great improvement of seismic imagery in the past ten years, new prospects have arisen. Mantle plumes are expected to be rather narrow, and their detection by seismic techniques requires specific developments as well as dedicated field experiments. Regional travel-time tomography has provided good evidence for plumes in the upper mantle beneath a few hotspots (Yellowstone, Massif Central, Iceland). Beneath Hawaii and Iceland, the plume can be detected in the transition zone because it deflects the seismic discontinuities at 410 and 660 km depths. In the lower mantle, plumes are very difficult to detect, so specific methods have been worked out for this purpose. There are hints of a plume beneath the weak Bowie hotspot, as well as intriguing observations for Hawaii. Beneath Iceland, high-resolution tomography has just revealed a wide and meandering plume-like structure extending from the core-mantle boundary up to the surface. Among the many phenomena that seem to take place in the lowermost mantle (or D″), there are also signs there of the presence of plumes.

In this article I review the main results obtained so far from these studies and discuss their implications for plume dynamics. Seismic imaging of mantle plumes is still in its infancy but should soon become a turbulent teenager.

ABOUT MANTLE PLUMES

What Are Plumes?

In 1963, with the emergence of plate tectonics, Tuzo Wilson (1963) remarked that the chain of Hawaiian volcanoes (Figure 1, see color insert) could be explained by the motion of the Pacific plate toward the northwest above a stationary hotspot. A few years later, Jason Morgan (1971) proposed that a thermal plume rising from the core-mantle boundary (CMB) was bringing up the hot material responsible for the hotspot. In convective systems, such plumes form naturally from thermal boundary layers through the Rayleigh-Taylor instability

(Figure 2). Subducting lithospheric slabs and hot plumes could be the two complementary features of mantle convection.

Today, many more hotspots have been identified, and much information has been obtained [see Duncan & Richards (1991) for a review, and Hofmann (1997) for a geochemical perspective]. In particular, it has been possible to estimate the buoyancy flux of most plumes by modeling their topographic and gravity swells (Davies 1988, Sleep 1990, Ribe & Christensen 1994). Figure 3 (see color insert) maps these fluxes and gives the names of a few hotspots.

Clearly, the distribution of hotspots is not random. Wide regions are devoid of hotspots, whereas the Pacific dominates the buoyancy flux. Many authors have emphasized the correlation between the hotspot distribution and other geophysical observables (geoid highs, low velocities in the deep mantle, etc) (see for example Weinstein & Olson 1989, Montagner 1994, Ribe & de Valpine 1994). I will not cover these issues but rather concentrate on individual plumes.

Despite talented but isolated opponents (Anderson 1995, 1998), the plume hypothesis is now widely accepted. However, many questions remain unanswered: Do plumes actually exist? What do they look like? How wide are they? How hot are they? Do they really rise from the core-mantle boundary? All of them? Are they tilted on their way up? Are there different kinds of plumes? Seismic imaging is the answer! Seismic travel-time tomography has provided spectacular images of subducting slabs (Grand 1994, van der Hilst et al 1997, Bijwaard et al 1998) that have had a profound impact on how we envision mantle convection.

The purpose of this article is to review the various efforts devoted to imaging mantle plumes using seismic waves. I give an overview of the main results obtained so far, and explain which tools are best suited to investigate the structure

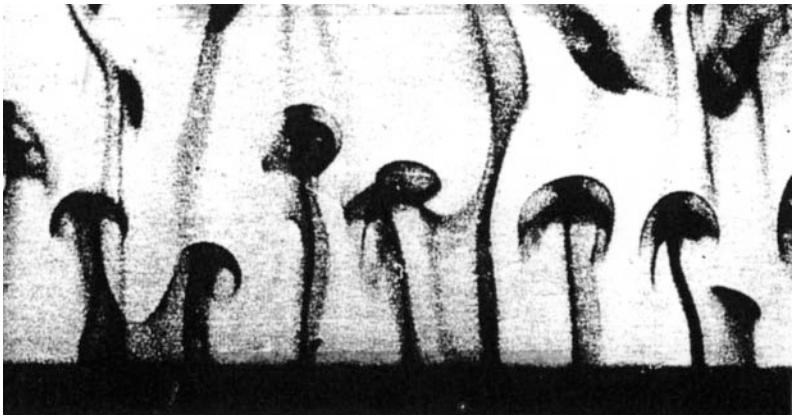

Figure 2 Thermal plumes rising from an unstable thermal boundary layer in water heated from below. The boundary layer has been colored, using an electrochemical technique. From Sparrow et al (1970).

of these objects. As a guide, let's first try to imagine what a thermal plume should look like in the Earth's mantle.

What Could Plumes Look Like?

In the Earth's mantle, viscosity decreases strongly when temperature increases. Laboratory experiments on isolated thermal plumes in a fluid with the same property reveal that the plume takes the shape of a mushroom: A large spherical head rises slowly while it is refilled with hot material rising more rapidly in the stem (Whitehead & Luther 1975, Olson & Singer 1985, Griffiths & Campbell 1990). As the head reaches the surface, it flattens off and spreads horizontally. We are still lacking a complete geodynamical model of a mantle plume; nevertheless, we can sketch the main features of such an object, with emphasis on the features that can be imaged with seismological tools (Figure 4).

Starting from the top, we find a wide cushion of plume material ponding beneath the lithosphere. The analysis of hotspot swells indicates that this cushion spreads laterally more than 1,000 km in diameter, and is elongated in the direction of plate motion (Davies 1988, Sleep 1990). From petrological arguments, the maximum temperature in the Hawaiian plume at these depths is inferred to be about 250 K above that of ''normal'' mantle (McKenzie 1984, Watson & McKenzie 1991). Similar excess temperatures are proposed for Iceland and several other hotspots (Schilling 1991). In the uppermost mantle, an excess temperature

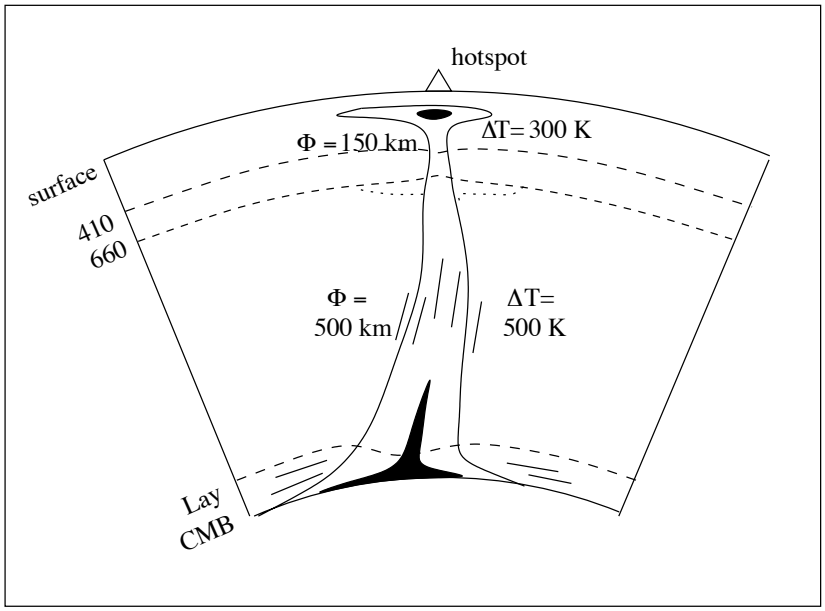

Figure 4 A sketch of what a mantle plume could look like. See text for description.

of 250 K yields P- and S-wave velocity anomalies of -2.25% and -2.75%, respectively, using the temperature derivatives adopted by Nataf & Ricard (1996).

Melt is present down to a depth of about 120 km (Watson & McKenzie 1991). The radial temperature distribution in the plume can be approximated as gaussian. We define the diameter Φ of the plume as twice the radius where the temperature excess has dropped to $1/e$ of its maximum value ΔT. Φ could be on the order of 150–200 km in the upper mantle.

Farther down, the plume crosses the two major seismic discontinuities at 410 and 660 km depth. They correspond to phase transitions of mantle minerals. As I discuss later, their Clapeyron slopes could be such that the 410-km discontinuity should be downwarped in the plume, while the 660-km discontinuity would be uplifted, resulting in a thinner-than-normal transition zone (here defined as the layer between the two discontinuities). Ponding could take place beneath the 660 km discontinuity (dotted line in Figure 4).

In the lower mantle, the viscosity is probably about 30 times higher than in the upper mantle (Richards & Hager 1984, Ricard et al 1989, Lambeck et al 1996). Thus the diameter of the plume should be larger, maybe 500 km or more (Albers & Christensen 1996).

In our sketch, the plume is rooted in a thermal boundary layer above the CMB. The temperature increase across this boundary could be as high as 1,000 K (Boehler 1993). The temperature excess in the plume could be on the order of 600 K in the lower mantle (Albers & Christensen 1996, Farnetani 1997).

Melt could be present both in this bottom thermal boundary layer (Williams & Garnero 1996, Zerr et al 1998) and in the stem of the plume that rises from it. If the Lay discontinuity (Lay & Helmberger 1983) at the top of D″ marks a phase transition (Nataf & Houard 1993), it could be deflected in the hot plume. In our sketch, it is drawn deflected downward, as recently proposed by Sidorin et al (1999).

Of course, the flow of hot material is nearly vertical everywhere in the plume, except near the top and bottom boundaries. This could result in preferential alignment of minerals, which can induce anisotropy of seismic wave propagation. Also, note that the plume is rising in a mantle where large-scale convective motions are present. It is thus expected to be deflected by the ''mantle wind'' (Olson & Singer 1985, Richards & Griffiths 1988). Realistic global mantle circulation models (Steinberger & O'Connell 1998, Corrieu & Ricard 1999) predict that the root of a plume can be offset horizontally up to about 1,500 km away from its surface expression.

The sketch of a mantle plume that I have drawn is very subjective and is intended only as a guide to help focus the various seismological instruments on this particular target. It turns out that the type of tool that can be used depends mostly on the depth range of investigation. Therefore, I have chosen to organize this review into four parts corresponding to four depth intervals: upper mantle (0–400 km depth), transition zone (400–700 km), lower mantle (700–2,700 km), and lowermost mantle or D″ (2,700–2,900 km). I will also mention a few unex-

pected findings at the end. Figure 5 (see color insert) is a summary map of the studies I present in this review, with symbols that indicate the relevant depth interval.

IMAGING PLUMES IN THE UPPER MANTLE (0–400 KM)

Global Survey from Surface Waves

Surface waves (Love and Rayleigh) are well suited for probing the uppermost mantle on a global scale. Although the stems of plumes are too narrow to be seen, the expected large diameter (~1,000 km) of ponds of plume material (which are responsible for the topographic and gravity swells) beneath the lithosphere could be detected in high-resolution studies. In their regional tomographic study of Africa, Hadiouche et al (1989) found hints for a large pond of slow material feeding several African hotspots and the East African rift. The global tomographic model of Zhang & Tanimoto (Anderson et al 1992, Zhang & Tanimoto 1993) displays plume ponds associated with several hotspots (Hawaii, Iceland, Azores, Tristan, Afar). Additional evidence was brought by regional studies (Roult et al 1994).

Rayleigh waves with a period of 75 s are particularly sensitive to heterogeneities just below the lithosphere. Global maps of the phase velocity of these waves are normally dominated by long-wavelength variations, which are caused by the thickening of the lithosphere with age. In Figure 6 (see color insert), I have tried to remove this signal by retaining only spherical harmonic degrees l from 10 to 40 (i.e. wavelength of the heterogeneities smaller than 4,000 km) of the model obtained by Ekström et al (1997).

Localized slow structures are present and seem to correlate with hotspot locations (Iceland, Azores, Canaries, Tristan, Bouvet, Crozet, Afar, Easter, Fernandez, Galapagos, etc). However, the correlation is far from perfect. In particular, Hawaii, despite its impressive topographic and gravity swell, does not show up clearly as a slow region. This is possibly an artifact, given that these global surface wave studies rely on permanent long-period seismic stations, which are a very long distance apart in the Pacific. As you will see later in this section, evidence for slow material ponding beneath Hawaii is just emerging from more regional studies.

Regional Studies

I will now concentrate on the imaging of the stem of plumes in the upper mantle. This depth interval is the realm of regional travel-time tomography: Install an array of seismographs on a hotspot, record as many earthquakes as possible (usually at teleseismic distances: epicentral distance larger than 30°), measure the arrival times of P- (and S-) waves across the array, subtract the times predicted using a radial reference model, and invert these residual times to build an image

of the lateral variations of seismic velocities from the surface to a maximum depth that depends upon the aperture of the array.

One then faces a dilemma: Either target a ''nice'' hotspot, such as Hawaii or La Réunion, with well-defined characteristics (age progression of the volcanoes along a linear chain, swell, etc), and then encounter technical difficulties (small aperture of the array in the absence of ocean-bottom seismometers, noisy stations, remote earthquakes, etc); or, investigate a continental hotspot with much better seismological conditions, but with rather ill-defined hotspot characteristics [mostly because of the more complex nature of the continental lithosphere, which plume material had to get through (e.g. Ebinger & Sleep 1998)]. The two cases have been treated, and I review the main results.

Continental Hotspots

Yellowstone Yellowstone (USA) was the first continental hotspot to receive a dedicated field experiment (Iyer et al 1981). Some 50 short-period seismographs were installed in and around the Yellowstone caldera. The aperture of the array was about 200 km. The tomographic inversion reveals slow P-wave velocities beneath the Caldera, down to the base of the model at a depth of 100 km. The anomaly reaches -5% and is about 50 km in diameter.

The survey was extended to the southwest with the deployment of two northwest-trending linear arrays of 15 seismographs across the Snake River Plain, which ennabled resolution to a somewhat greater depth (Evans 1982). The results indicate 2% slow material down to the base of the model at 350 km depth. Yellowstone has been recently revisited, and a better tomographic model has been derived (Saltzer & Humphreys 1997). A northwest-southeast cross section is shown in Figure 7 (see color insert), and shows good agreement with the earlier model of Evans. The authors emphasize that they do not find evidence for a wide cushion of slow material ponding beneath the lithosphere, but rather a thin conduit of low velocities extending down to at least 300 km.

Massif Central Massif Central (France) is the site of recent volcanism and is thought to be a hotspot (Froidevaux et al 1974). It was selected for a detailed seismic tomography experiment, which was conducted in 1991–1992 (Granet et al 1995a). Some 80 short-period seismographs were deployed across the Massif Central, complementing 22 permanent stations. The aperture of the array was about 300 km, with spacing as small as 15 km between stations. Some 42 teleseismic events were recorded. A P-wave velocity model was constructed, with resolution down to 270 km. The results (Granet et al 1995a,b), illustrated in Figure 8 (see color insert), show a cylindrical slow region extending from the surface to the base of the model. Its diameter is about 200 km, and the P-wave velocity anomaly reaches -2.5%.

Eifel Another potential European hotspot is receiving considerable attention at the moment: the Eifel hotspot in northern Germany. Early tomographic studies (Raikes & Bonjer 1983) showed low P-wave velocities in the uppermost mantle beneath the Rhenish Basin. In the new experiment, more than 150 seismographs have been deployed. The array spans nearly 500 $\times$ 500 km and is centered on the Eifel volcanics (Ritter et al 1997, 1998). Two hundred teleseismic earthquakes have been recorded between November 1997 and June 1998, and data treatment is in progress at the time of writing (see http://www.uni-geophys.gwdg.de/~eifel). Note that the survey also includes other methods of investigation (electromagnetic, gravity).

Oceanic Hotspots

Hawaii Hawaii is probably the most typical hotspot. Unfortunately, its position in the middle of the Pacific, far away from earthquakes and seismic stations, makes imaging problematic. Nevertheless, it was the target of one of the first tomographic studies, performed by Ellsworth (Ellsworth 1977, Ellsworth & Koyanagi 1977), using the local array of seismographs installed for volcanic monitoring. Because all stations are on the island itself, the aperture of the array is small and limits the depth of investigation to less than 150 km. In effect, this means that one can only image the ''magma tubing'' that crosses the lithosphere and feeds the volcanoes. In their pioneering study, Ellsworth & Koyanagi were extremely careful in their interpretation of the images they obtained.

Recently, new and better images have been obtained by Tilmann (1999). He used essentially the same stations and earthquake distribution as Ellsworth & Koyanagi, but took advantage of 20 years' worth of progress in data acquisition, data analysis, and tomographic inversion. His results show a northwest trending 3% slow anomaly across the island of Hawaii, which seems to split into more patchy blobs below about 80 km.

As nice as they are, these images shed no light on the existence of a plume beneath Hawaii. One probably needs to wait for the deployment of ocean-bottom broad-band seismographs around Hawaii, which is currently under way (K Priestley, personal communication; Laske et al 1999; see http://mahi.ucsd.edu/Gabi/swell.html), before getting an idea of the structure of the Hawaiian plume in the upper mantle.

However, I should mention a nice experiment conducted by Priestley & Tilmann (1999), which brings valuable information concerning the top of the Hawaiian plume. Taking advantage of a local array of broad-band seismographs installed on Hawaii since 1994, these authors could measure the dispersion of surface waves on the short path between the local array and the permanent station of Kipapa (Geoscope, IRIS) on the island of Oahu (see Figure 1). This investigation nicely complements an earlier surface wave dispersion study between Oahu and the island of Midway (Woods et al 1991, Woods & Okal 1996). Rayleigh waves with periods between 20 and 80 s are clearly slow along the Oahu-Hawaii path.

Priestley & Tilmann obtained the two profiles shown in Figure 9 (see color insert) for the two different paths. The comparison yields S-wave velocities that are some 5% lower than normal beneath the Hawaiian swell, down to a depth of 200 km. The preliminary results from the *SWELL* pilot-experiment (Laske et al 1999) also seem to indicate S-wave velocities lower than normal at these depths beneath the swell. These near-field surface wave analyses could prove useful in other situations; However, I should note that they may require using higher order theories than the simple great-circle average analysis (Maupin 1992, Lognonné & Romanowicz 1990, Neele et al 1989).

Somewhat more elaborate is the method developed by Capdeville et al (1999). The authors investigated how plume-like heterogeneities can scatter surface waves. Using a normal mode formalism and the Born approximation, they developed a comprehensive analysis of the forward problem. They showed that, for realistic plume parameters, the amplitude of the scattered waves is small (2% to 10%). In addition, the fundamental mode of the surface waves will probably be more affected by the cushion of slow material than by the stem of the plume. An application to real data targeting the Hawaiian plume did not yield conclusive results (E Stutzmann, personal communication).

Iceland Because the Iceland hotspot sits on the Mid-Atlantic ridge, it has developed a 15-km-thick crust, so that Iceland is a much bigger island than Hawaii. Thus it provides a much better geometry to investigate the upper mantle beneath it, even though the seismic noise level is rather high. The first images of the Icelandic plume were obtained by Tryggvason et al (1983), using the local array of 39 short-period seismographs. The authors constructed a P-wave velocity model, which displays a ~2.5% low velocity cylindrical region, about 200 km in diameter, extending down to 350 km. More recently, a dedicated experiment called *ICEMELT* was carried out. Between 1993 and 1996, 15 broadband seismic stations recorded 86 earthquakes (Bjarnason et al 1996a,b). Wolfe et al (1997) presented images for both P- and S-waves (see Figure 10, color insert). The P-image confirms the earlier results and clearly shows a cylindrical 2% slow anomaly extending down to about 400 km. The S-image is similar, with a maximum slow anomaly of 4%. Wolfe et al tried to interpret their results in terms of a temperature excess in the plume and diameter, and claimed that they can exclude the low-temperature, large-diameter end of the geodynamical models. Namely, they obtained $\Delta T = 250$ K and $\Phi = 300$ km.

This effort indicates a promising method of research, in which direct comparison is drawn between tomographic models and various geodynamical observations. However, it is notoriously difficult to trust the amplitudes of velocity heterogeneities derived only from delay-time tomography, so progress in this direction probably requires more specific methods. One example is the near-field surface wave study performed by Priestley & Tilmann (1999) for Hawaii, as already mentioned. The same group (Tilmann et al 1998) has examined the effect of a vertical cylindrical slow anomaly on the seismic waves that interact with it.

The authors solved the full wave equation for a homogeneous background medium, and found that the main diagnostic observation that would indicate the presence of a plume is the appearance of a transverse component to the P-wave, which is absent when there is no plume. The amplitude of this component reaches 25% of the radial component if the station is situated a few plume radii behind the plume, and could be observed when the signal-to-noise ratio is high. Another remarkable property is a strong modulation of the amplitude of the ''direct'' P-wave as a function of the azimuth from the plume, in its ''shadow,'' as a result of focusing effects.

This modulation is frequency dependent. Allen et al (1999) took advantage of this property to try to better locate and calibrate the Iceland plume. They observed strong variations of t^* for various Iceland seismic stations, depending on the azimuth of the incoming teleseismic S-waves. The t^* parameter provides a measure of the relative amplitudes of high-and low-frequency components, with larger t^* indicating larger attenuation along the path of the seismic wave. Allen et al computed synthetic t^* patterns for a cylindrical plume in a homogeneous background, by solving the wave equation by finite difference in two dimensions. As shown in Figure 11 (see color insert), there appears to be a rough correspondance between the t^* observations and the patterns predicted for a rather narrow and ''strong'' plume ($\Phi = 200$ km, $\Delta V_S = 12\%$). Allen et al note that such a strong anomaly would produce an integrated time delay for S-waves larger than observed, but they argue that an actual S-wave with finite frequency will get a much reduced delay, because of the ''healing'' of the wavefront (Wielandt 1987) behind the plume. I will come back to this effect in a later section.

To conclude this section, one can say that there is good evidence of plume-like slow structures in the upper mantle beneath several hotspots, both continental and oceanic. Typical diameters range between 100 km and 300 km, with P-wave maximum slow anomaly from 2% to 4%, and S-wave maximum slow anomaly from 4% up to 12%. The translation in terms of a temperature anomaly is not trivial (and may be an oversimplification). Most authors mention that their results are compatible with a temperature excess on the order of 300 K, which in turn is compatible with current petrological and geochemical estimates.

Most evidence comes from dedicated regional travel-time tomography. In the depth range that can be resolved (0–400 km), the detection of a plume does not answer many of the questions concerning the origin of plumes. Nevertheless, it is in this depth range that quantitative correlations with other observables (petrological, geochemical, gravimetric, etc) will be most fruitful.

In addition to being only relative, the amplitude of velocity-anomalies is not well determined in regional travel-time tomography. Therefore, it is important that techniques providing improved resolution be developed and applied to real data. The Hawaiian hotspot, and other prominent oceanic hotspots such as La Réunion or Cape Verde, deserve dedicated seismic campaigns with broad-band ocean-bottom instruments.

IMAGING PLUMES IN THE TRANSITION ZONE (400–700 KM)

Hints from High-Resolution Global Tomography

Figure 12 (see color insert) shows the lateral heterogeneities of S-wave velocities in the transition zone from the recent high-resolution tomographic model of Grand (Grand 1994, Grand et al 1997). Grand has carried out an impressive study of the waveforms of S-wave and its multiples (SS, SSS, etc), which enabled him to map small-amplitude and relatively small-scale features throughout the mantle. In the transition zone, his model nicely recovers high-velocity regions that indicate the presence of subducted slabs. But there is also some evidence for more spot-like slow regions, which can be associated with hotspots (Iceland, Azores, Bermuda, Bouvet, Afar, Hoggar, Louisville, Samoa, Pitcairn, etc). As for the uppermost mantle, the correlation is not perfect. Note that, again, resolution is poor at these depths in the Pacific, particularly near Hawaii. Also note that even in these high-resolution images, the smallest features that can be imaged have diameters on the order of 1,000 km, quite a bit larger than the expected dimensions of plume stems at these depths.

Regional Studies with Receiver Functions

There are two major seismic discontinuities in the mantle, at depths of about 410 km and 660 km. They are a result of solid-state transitions of the major minerals of mantle rocks. The 410-km seismic discontinuity corresponds to the transition from olivine to β-spinel, whereas the 660-km seismic discontinuity is controlled by the transition from γ-spinel to pervoskite and magnesowustite. To simplify, the 410-km discontinuity marks an endothermic phase transition and should thus be deflected downward in a hot plume; the 660-km discontinuity is exothermic and would be deflected upward. Because of the associated negative buoyancy force, the 660-km discontinuity could inhibit the ascent of plumes from the lower to the upper mantle. The reality is certainly more complex, as other phase transitions also contribute and could even annihilate the buoyancy effect produced by the sole γ-spinel transition (Weidner & Wang 1998). In any case, it would be very useful to see if any ''plume signature'' exists in the transition zone beneath hotspots.

The idea is to use the seismic discontinuities themselves as markers, and to search for bumps on them. Early attempts in the region of Hawaii by Neele & Snieder (1991) using long-period $P_{410}P$ waves, which bounce on the lower side of the 410-km discontinuity, did not provide conclusive results. This is not surprising, because the Fresnel zone of these waves (the horizontal patch they sample on the discontinuity) is an order of magnitude wider than the expected diameter of the plumes.

More recently, several interesting results have been obtained using the ''receiver function'' technique. The idea, sketched in Figure 13, is that a P-wave can convert into an S-wave at either discontinuity (*d*) on its way up to a seismic station. These P_ds are best seen on the component of ground motion that is perpendicular to the direct P ray and in the vertical plane (SV). By stacking (summing) this component of broad-band seismograms corresponding to different teleseismic earthquakes, with appropriate move-out, one can detect and analyze these converted waves (e.g. Vinnik 1977, Paulssen 1988). If a small-aperture array of stations is available, a better signal-to-noise ratio is obtained (Kind & Vinnik 1988).

When both $P_{410}s$ and $P_{660}s$ are observed, the time difference between the two arrivals provides a good measure of the thickness of the transition zone in the region beneath the station, with a lateral resolution better than a couple of hundred kilometers, depending on the azimuthal distribution of earthquakes used in the stack.

Iceland The receiver function technique was applied to Iceland by Shen et al (1998), using the *ICEMELT* array of 14 portable broad-band stations (Bjarnason et al 1996a,b). They found that the transition zone is about 230 km thick beneath

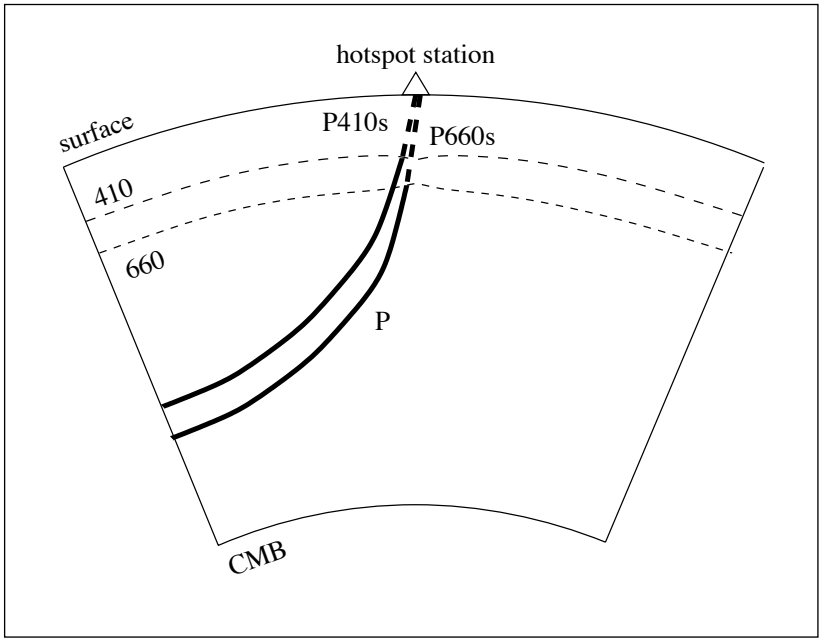

Figure 13 P-waves convert to S-waves at seismic discontinuities at depths of 660 and 410 km, yielding waves $P_{660}s$ and $P_{410}s$, which can be observed on the radial component of displacement at the surface (the horizontal component in the plane of the figure).

central and southern Iceland (see Figure 14, color insert). This is about 20 km less than in ''normal'' mantle which suggests, in agreement with the sketch of Figure 4, that the two seismic discontinuities are indeed deflected in the hot plume.

Hawaii A similar study was carried out by Li et al (1999) for Hawaii. They compared the results obtained from an array of broad-band stations situated on the main island of Hawaii to those derived from records of the permanent station of Kipapa on Oahu (see Figure 1). The converted $P_{660}s$ wave is not very clear for the stations on Hawaii, but the records seem to indicate that the transition zone is 30 to 40 km thinner beneath Hawaii than beneath Oahu, which does not deviate from ''normal'' mantle.

Vinnik et al (1997) documented another effect. By comparing the receiver functions of several permanent stations of the Geoscope and IRIS networks in the Pacific, they observed that for some stations, the pulse of $P_{660}s$ is broadened by up to 3 s with respect to ''normal'' behavior, whereas $P_{410}s$ pulses are essentially all identical. The stations that display broadening are RAR (Raratonga), PPT (Tahiti), and RPN (Easter), which are in the south Pacific superswell region (McNutt & Fischer 1987). Vinnik et al speculate that this broadening is due to a smearing of the 660-km discontinuity over 100 km, which indicates the presence of slow material ponding beneath the discontinuity. Recent experimental results by Weidner & Wang (1998) suggest an alternative explanation. These authors find that the 660-km phase transitions spread over more than 50 km for mantle temperatures above 2,100 K. The observations of Vinnik et al could therefore indicate temperatures roughly 200 K higher than normal in the superswell region. The link with individual plumes feeding Tahiti, Easter, and the Marquesas remains to be found. Note that Li et al (1999) also found a broadened $P_{660}s$ pulse beneath Hawaii.

Shen et al (1998) claimed that their observation of a thinner-than-normal transition zone beneath Iceland demonstrates that the plume comes from the lower mantle. Li et al (1999), who found an even thinner transition zone beneath Hawaii, essentially reached the same conclusion. A definite statement on this issue will probably require more complete seismological modeling and the exploration of alternative interpretations. It will also be interesting to see if this is really a feature of all hotspots. In any case, one can assume that these results strongly suggest a lower mantle origin for both Iceland and Hawaii. Later in this article, I mention other observations that lend support to this view.

IMAGING PLUMES IN THE LOWER MANTLE (700–2700 KM)

Several questions on the origin of hotspots would find the beginning of an answer if plumes were detected in the lower mantle. The lower mantle was the first layer of the Earth to be imaged in global tomography (Dziewonski 1984), and recent

models have reached an amazing resolution (van der Hilst et al 1997, Grand 1994, Grand et al 1997, Bijwaard et al 1998). It would thus seem logical to look in these models for evidence of plumes beneath hotspots—and in fact, such evidence is starting to emerge (Bijwaard & Spakman 1999, Goes et al 1999). However, the Fresnel zone of a short-period P-wave deep in the lower mantle is about 400 km in diameter; this gives the lower limit of the size of objects that can be imaged by travel-time tomography in the lower mantle. The situation is even worse for slow and cylindrical objects, such as plumes, because the wavefront can ''heal'' quickly after traversing the slow cylinder, thereby severely reducing the amplitude of the time-delay (Wielandt 1987, Gudmundsson 1996, Allen et al 1999, Dahlen et al 1999, Hung et al 1999). Therefore, plumes with expected diameters of about 400 km in the lower mantle could be totally invisible in classical travel-time tomography.

To address this problem, researchers have developed two strategies. The first one consists of selecting a region, a geometry, and data so as to lower the size of the Fresnel zone as much as possible. This led Nataf & VanDecar (1993) to carry out a detailed analysis of P-waves that traversed a hypothetical lower mantle plume beneath the Bowie hotspot.

The other possibility is to go beyond travel-time tomography and use more resolving waveform analysis methods. This approach was taken by Ji & Nataf (1998a,b), who investigated the properties of long-period P-waves scattered by plume-like structures, then built a suited variant of diffraction tomography and applied this new method to imaging the Hawaii plume.

Bowie The Bowie hotspot, near the west coast of Canada, is certainly not a spectacular hotspot. The Bowie seamount is at the end of a northwest-trending linear chain of volcanic seamounts, which show a reasonable age progression (Turner et al 1980). There is no clear topographic swell present, which indicates that the buoyancy flux of the potential plume is small—between 0.3 Mg s^{-1} (Sleep 1990) and 0.8 Mg s^{-1} (Davies 1988), more than one order of magnitude smaller than for Hawaii (see Figure 3).

The Bowie hotspot was chosen as a target by Nataf & VanDecar because of its exceptional situation: It lies right in the middle between the Alaskan subduction zone, which provides well-behaved frequent seismic sources, and the Washington regional seismic network of short-period seismographs. The epicentral distances are between 25° and 30°, so the seismic rays intersect the hypothetical plume at their bottoming point, just below the 660-km discontinuity.

In this geometry, the half-period Fresnel zone of 1 s period P-waves is only about 250 km wide. Also, because the stations are only about 1,000 km behind the expected plume, wavefront healing cannot completely remove the plume time delay (Nataf & VanDecar 1993).

The detailed analysis of P-wave time delays (using multi-channel cross-correlation) reveals that rays that travel about 150 km northeast of the hotspot position are slowed down by about 0.15 s, over a width of ~150 km. This led Nataf

& VanDecar to speculate that they had detected a mantle plume beneath Bowie at a depth of about 700 km. The very small observed time delay was compatible with a temperature excess of about 300 K in a 150-km diameter plume.

Despite all precautions used, the width of the Fresnel zone is a bit larger than the diameter of the detected plume. It is therefore likely that an interpretation in terms of ray propagation is not quite correct. Recently, Dahlen et al (2000) developed a theory to compute, in the single-scattering Born approximation, the sensitivity or Fréchet kernels for time-delays measured by cross-correlation. Applications to the effect of a simple Gaussian-shaped spherical slow anomaly (Hung et al 2000) show that the ray-theory bell-shaped time-delay pattern is replaced by a smaller-amplitude curve having two bumps when the size of the object is small with respect to the Fresnel zone (see their figure 7a). Although a more complete application of their banana-doughnut theory to the Bowie geometry remains to be done, one can try to reinterpret the travel-time curve of Nataf & VanDecar in the light of these results. Tentatively, the equivalent ray-theory bell-shaped curve that could explain the observations would imply a somewhat wider plume ($\Phi = 300$ km), with a higher temperature excess ($\Delta T = 400$ K), and the plume would be centered on the hotspot position.

The Bowie hotspot was also probed with the method discussed next for Hawaii, but no coherent anomaly was found across the lower mantle (Ji 1996).

Hawaii The Earth's major hotspot, Hawaii, is too far away from earthquakes and stations to apply the preceding technique. In fact, the lower mantle beneath Hawaii is not resolved at all in global tomography down to a depth of about 2,000 km (van der Hilst et al 1997). Hence came the need for more appropriate techniques. This motivated the study of Ji & Nataf (1998a), who investigated the properties of the seismic waves that are scattered by a plume-like structure. Scattered P-waves arrive after the direct P-wave, and can be observed even when the direct ray is not traversing the plume. For a vertical plume, the scattered P-wave is an Airy phase, which collects scattered energy from all the slices of the plume that lie within the Fresnel zone of the P-wave that would hit the plume, if the source-plume-station path were unfolded. Ji & Nataf modeled the scattered waves within the single-scattering Born approximation, using ray theory. They found that the amplitude of 20 s-period scattered P-waves for realistic geometries and for a typical thermal plume ($\Delta T = 600$ K, $\Phi = 400$ km) would reach only about 2% of the amplitude of the direct P-wave.

In principle, the use of scattered waves permits a much better spatial resolution than is achievable in delay-time tomography. In fact, diffraction tomography probes the ''sides'' of the Fresnel zone, for which a given time separation δt translates to a much smaller distance than in the center of the Fresnel zone, which corresponds to a minimum of the travel time. The price to pay is that a given arrival could be due to a scatterer located anywhere on an ellipsoid—that is, related to the Fresnel zone, so that the location of the scatterers can be ambiguous. However, if one uses many waveforms, one can invert and image the actual

scatterers; this is the essence of diffraction tomography (e.g. Devaney 1984, Revenaugh 1995, Lay & Young 1996). A positive aspect of the plume application is that the problem is reduced to two dimensions for a vertical plume.

Despite the very small predicted amplitudes, Ji & Nataf (1998b) applied this new method to imaging the region beneath Hawaii, which was found to be well sampled (the hit count of $1^\circ \times 1^\circ$ cells was between 50 and 200). The surprise was that they found a high level of scattered energy (more than 15%), which seemed to come mostly from a spot situated a few degrees northwest of Hawaii (Figure 15, color insert). Such an amplitude would imply a much larger scattering anomaly than modeled, probably more than 20% P-wave velocity anomaly. Given that the depth range sampled in this study is the lower 1,000 km of the lower mantle, strong anomalies could be produced by partial melt in the stem of the plume (see Figure 4), because the ultra low-velocity zones at the very base of the mantle (see Garnero 2000) also require extremely low velocities (10% for P-waves and maybe 30% for S-waves). Nonetheless, one cannot dismiss the possibility that the observed scattered energy has another origin than the modeled one, so further analysis is required.

Iceland The diffraction tomography method presented above was also applied to Iceland (Ji 1996). The hit count for $2^\circ \times 1^\circ$ cells was between 70 and 200. As shown in Figure 16 (see color insert), a strong scattering slow region was found a few degrees northeast of Iceland. Again, the amplitude was much greater than predicted for a simple thermal plume, and the same caution applies.

Recently, Bijwaard & Spakman (1999) have found, in their global high-resolution tomographic P-wave model, some evidence for a slow region extending across the entire mantle beneath Iceland (Figure 17, color insert). The anomaly reaches only 0.5% (which could translate into $\Delta T = 150$ K). It sweeps across the mantle (maybe the effect of ''mantle wind'') and measures up to 1,000 km in diameter.

The same group (Goes et al 1999) proposed that this imaged plume, which is quite wide, is connected to two other zones of slow velocities at depths between 1,100 and 1,700 km. These zones lie beneath the Canary islands and Central Europe. The latter could be related to hotspot activity in the Eifel and Massif Central.

Other attempts at imaging plumes in the lower mantle using seismic waves that propagate steeply in the mantle (such as the core-reflected waves PcP and ScS or core-transmitted waves PKP and SKS), were not conclusive. Helffrich & Sacks (1992) could not find significant travel-time anomalies for PKP waves recorded at hotspot stations.

A very large travel-time delay (20 s) reported for an ScSScS wave with a surface bounce point beneath the Trinidade hotspot (Okal & Anderson 1975) was shown to be a result of a phase misidentification (Nataf et al 1981). In fact, there is little hope of using core-reflected or core-transmitted waves to detect plumes

in the lower mantle because the phenomenon of wavefront healing mentioned before is very significant in this geometry.

IMAGING PLUMES IN THE LOWERMOST MANTLE (2700–2900 KM)

The lowermost mantle is another region where, as in the uppermost mantle, we expect that plume signatures could be rather pronounced and larger in scale. Indeed, if plumes originate from this region, they tap hot material from a wide zone at the base of the mantle. Therefore, one might expect slow zones with diameters on the order of 1,000 km or more. Also note that, as we go deeper into the mantle, it is more difficult to know where the signature of a given hotspot should be located, since it could be displaced by more than 1,000 km under the action of the ''mantle wind'' (Steinberger & O'Connell 1998, Corrieu & Ricard 1999).

The lowermost mantle is also a region where many complex phenomena take place, and for which many different seismological tools have been applied [see the review by Garnero in this volume (Garnero 2000)]. You will see that the recently discovered ULVZ (Ultra-Low Velocity Zones) at the very bottom of the mantle are found preferentially under hotspots. In this section I also report on regional studies that give evidence for a deep origin for two of the most studied hotspots: Hawaii and Iceland.

Global Overview with Ultra-Low Velocity Zones

Evidence for very low P-velocities at the base of the mantle was found through a detailed analysis of SP_dKS waveforms (see Figure 1 of Garnero 2000) (Garnero & Helmberger 1995, Garnero et al 1998). This could imply reductions in P-wave velocities of up to 10%, which have been attributed to the presence of partial melt (Williams & Garnero 1996). Now that the search for ULVZ has been extended to a large portion of the globe, researchers can look for a possible correlation with hotspot locations. This was taken up by Williams et al (1998), who did find a correlation. Figure 18 (see color insert) compares the locations of ULVZ with hotspot fluxes. The link with individual plumes is not obvious yet, but this correlation certainly gives support to the idea that hotspot plums originate from the base of the mantle.

Regional Studies

Hawaii Only a few years after Jason Morgan's mantle plume hypothesis (Morgan 1971), seismologists reported evidence for a core-mantle boundary source for the Hawaiian volcanic chain. In a series of articles (Kanasewich et al 1972, 1973; Kanasewich & Gutowski 1975), Kanasewich et al detailed a high-velocity anomaly lying in the lowermost mantle, a few degrees northeast of Hawaii. The

P-wave anomaly, which reached 10%, was deduced from an analysis of the phase velocity of direct and core-diffracted P-waves across two short-period seismic arrays in Canada. The reality of this anomaly was disputed by Wright (1975). Wright argued that such high velocities were not compatible with other observations for the same region, that the phase-velocity analysis was non-unique, and in particular that lithospheric structure beneath the seismic arrays could explain the reported anomaly. There was also some concern about the treatment of the P_{diff} waves used in Kanasewich's analysis. In their reply to Wright's comment, Kanasewich et al (1975) maintained their interpretation. Recent high-resolution P-wave models tend to show low velocities in the same region (see Figure 5 of Garnero 2000 in this volume). Retrospectively, one must acknowledge that the interpretation of Kanasewich et al was not completely well-founded.

In any case, this first attempt was followed by several others, for at least one good reason: The portion of the lowermost mantle in the Hawaii region sits in the middle of the path from the Tonga subduction zone (one of the most active seismic regions) to North America (which has one of the most active seismological communities).

Recently, Russell et al (1998) found evidence for rapidly varying S-wave velocities some 1000 km southeast of Hawaii. They also reported a change in the anisotropy of S-waves in the same region, which would be compatible with a flow pattern changing from subhorizontal away from the plume to subvertical within. The authors were not much concerned by the fact that the anomaly is quite far from Hawaii, because this is precisely what some ''mantle wind'' models predicted (Steinberger & O'Connell 1998).

However, the evidence still remains unclear since Bréger & Romanowicz (1998) did not find significantly low velocities in this region, but rather much farther away to the south. It is then tempting to link this anomaly to the South Pacific superswell rather than to Hawaii. In any case, it would be difficult to reconcile the results of Ji & Nataf (1998b), pointing to a plume a few degrees northwest of Hawaii, with those of Russell et al (1998) if the latter indeed relate to Hawaii.

Iceland We have already mentioned the work of Bijwaard & Spakman (1999). These authors found a P-wave velocity anomaly of about -0.5% that extends all the way from the surface to the core-mantle boundary beneath Iceland. In the lowermost mantle, the slow anomaly seems to be situated to the southwest of Iceland. A localized dome-shaped ULVZ has also been detected by Helmberger et al (1998). The dome could be 250 km in diameter and centered to the southeast of Iceland, in which case a shear-wave velocity anomaly as large as -30% is invoked. However, a strong trade-off exists, so a larger dome with a smaller velocity anomaly is also acceptable (Helmberger et al 1998).

On the theoretical side, specific methods are required to deal with the interaction of seismic waves with plumes in the lowermost mantle. In particular, waves that are diffracted by the core have a high potential but need to be treated with

appropriate methods. Recently, Emery et al (1999) worked out a method to treat the scattering of S_{diff} waves by heterogeneities in the Born approximation. Applications to plume-like structures show that an effect on the polarization of these waves is expected, but that this effect remains very small for a purely thermal plume.

UNEXPECTED FINDINGS

Although I have tried to give an optimistic and simple view on the prospect of seismic imaging of plumes, I have to mention a few studies that yield somewhat unexpected findings.

The first class concerns the evidence for a significant slow anomaly where plumes used to be, which we might call ''fossil plumes.'' The second study reports on faster-than-normal velocities associated with plumes, which I have named ''high-velocity plumes.'' Finally, I also give a few words on ''quiet plumes.''

Fossil Plumes

Paraná While they were conducting a regional tomographic study of part of the Brazilian shield with 10 broadband portable seismic stations spanning 800 km, VanDecar et al (1995) were surprised to find a cylindrical slow anomaly extending from the surface down to 500 km beneath the Paraná basin. The anomaly has a diameter of about 260 km, and maximum P-and S-wave velocity anomalies of -1.5% and -2%, respectively. The Paraná basin is covered with flood basalts 135 million years old, which seem to have erupted shortly before the opening of the South Atlantic ocean. It is thought that these flood basalts mark the arrival at the surface of the head of the mantle plume, which now feeds the Tristan da Cunha hotspot (see Figure 3) near the mid-Atlantic ridge (Morgan 1972, Campbell & Griffiths 1990).

What is surprising is that the mantle would retain a signature of this old event down to such a depth—not because it should have spread away under the action of thermal diffusion, since the maximum would only have dropped by a factor of 2, and its initial diameter would have been about 200 km. What is really surprising is that the stem remained vertical beneath Paraná during all that time, which seems to indicate that a thick mantle keel is attached to the moving South American plate, as proposed by Jordan (1975).

Deccan A similar observation has now been made for the Deccan in northwestern India (Kennett & Widiyantoro 1999). Regional P-wave tomography of India reveals a zone of low velocities beneath the Cambay graben. This area is at the northern end of the Deccan traps, which are impressive flood basalts that erupted 65 million years ago when the region was above the Réunion hotspot. Kennett & Widiyantoro observed a nearly cylindrical slow anomaly (1%, 300 km in diameter) extending from the surface down to about 250 km, where it seems

to connect to a wider and stronger slow anomaly extending down to more than 500 km depth. All this evidence suggests that we are seeing the remnant of the head of the Réunion plume, which got stuck below the Indian plate and has moved with it ever since.

Note that even over this long period of time, the temperature anomaly is not expected to have changed much as a result of thermal diffusion alone.

High-Velocity Plumes?

In a recent article, Katzman et al (1998) reported puzzling results that bear on plumes. The authors conducted a detailed study of a ''mantle corridor'' between the Tonga subduction zone and the Kipapa seismic station near Hawaii. The surprise is that they found high shear velocities in the upper mantle beneath regions of high topography associated with hotspot swells (including the Hawaiian swell). Not only that, but the authors also found low shear velocities in the Tonga subduction zone, where the old and cold Pacific plate is entering the mantle.

It is not easy to reconcile these observations with those obtained by other authors. As I mentioned, Priestley & Tilmann (1999) found 5% low shear velocities down to 200 km beneath the Hawaiian swell. The low velocities in the Tonga subduction zone are also at odds with results from global tomography (see Figure 12, for example). The method used by Katzman et al (1998) was developed by Zhao & Jordan (1998) and is very elaborate. Perhaps all trade-offs of the method have not yet been fully explored. The fact that the method assumes a 2-D structure and ignores azimuthal anisotropy could induce some artifacts.

Quiet (or Not Quite) Plumes?

Several regional tomographic models display plume-like low-velocity zones in regions where no hotspot is known at the surface. Three such zones are present in Kulakov's model for Siberia (Kulakov et al 1995), and a recent model of Tibet also shows one such zone (Wittlinger et al 1996). It could be that a plume exists there but is not hot enough to produce melt beneath the thick continental lithosphere (Ebinger & Sleep 1998, Albers & Christensen 1996). These observations also serve to remind us that regional relative travel-time tomography emphasizes lateral variations beneath the seismic array and is insensitive to any global vertical layering, thereby tending to produce cylindrical (or fan-like) features. Indeed, tomographic models derived from surface waves demonstrate that the mantle beneath Tibet is faster-than-normal down to a depth of 300 km (Griot et al 1998, Matte et al 1999).

DISCUSSION AND CONCLUSION

Hotspots hold the key to several crucial issues of mantle dynamics. In the multidisciplinary effort engaged to understand hotspots better, the first task assigned to seismologists was the detection of mantle plumes. Only ten years ago, this

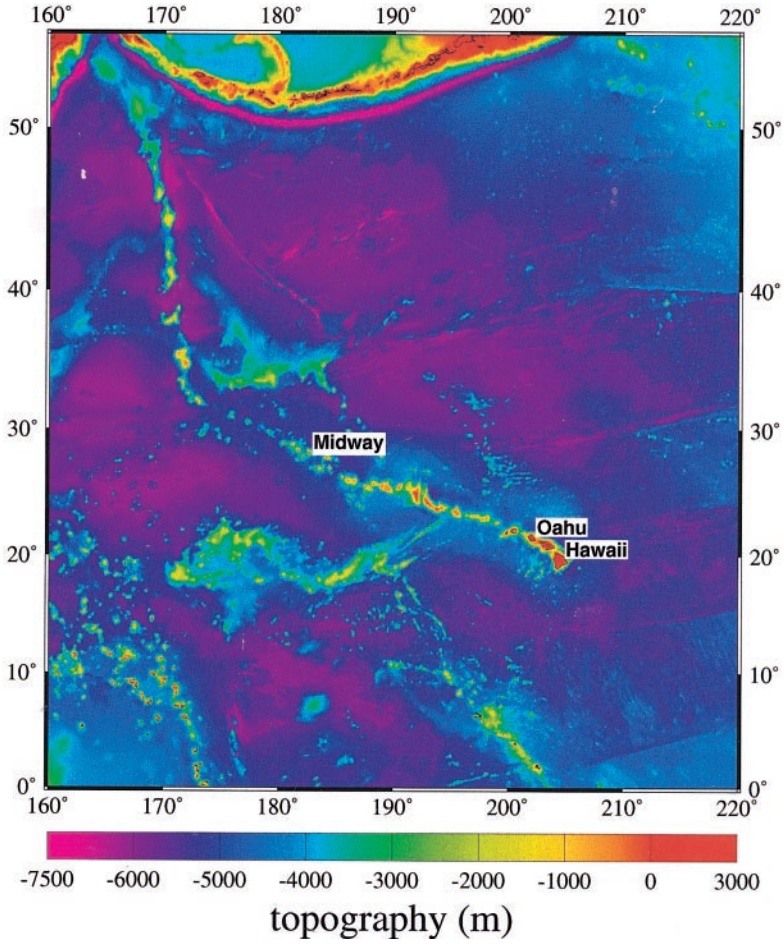

Figure 1 The Hawaiian volcanic chain as seen in the topography of the sea floor. The islands of Hawaii, Oahu, and Midway have been marked for reference in the text. Topography from ETOPO5 in Mercator projection. GMT (Wessel & Smith 1991) is the software used for this figure and several others.

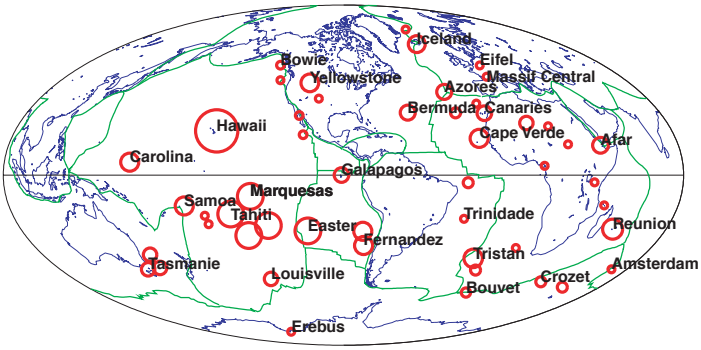

Figure 3 Buoyancy fluxes and names of hotspots. The surface of the red circles is proportional to the plume buoyancy flux estimated by Sleep (1990). Hawaii has the largest flux (8.7 Mg s–1). Flux could not be estimated for the hotspots drawn with the smallest symbols. Plate boundaries are drawn in green. The same Hammer projection centered on longitude 90 W is used for all global maps in this review.

Figure 5 (Next page) Summary map of studies on imaging plumes discussed in this review. The symbols indicate the depth range imaged, as given at the bottom of the figure, and their color specifies the type of observation. **Global map**: Massif Central (Granet et al 1995a,b); Eifel (Raikes & Bonjer 1983; Ritter et al 1997, 1998); Yellowstone (Iyer et al 1981, Evans 1982, Saltzer & Humphreys 1997); Tahiti and Rarotonga (Vinnik et al 1997); Bowie (Nataf & VanDecar 1993); Trinidade (Okal & Anderson 1975, Nataf et al 1981); Paranà (VanDecar et al 1995); Deccan (Kennett & Widiyantoro 1999). **Hawaii map**: 1 (Ellsworth 1977, Ellsworth & Koyanagi 1977); 2 (Tilmann 1999); 3 (Priestly & Tilmann 1999); 4 (Laske et al 1999); 5 (Vinnik et al 1997); 6 (Li et al 1999); 7 (Ji & Nataf 1998b); 8 (Kanasewich et al 1972, 1973; Kanasewich & Gutowski 1975); 9 (Russell et al 1998); 10 (Bréger & Romanowicz 1998); 11 (prediction: Steinberger & O'Connell 1998); 12 (prediction: Corrieu & Ricard 1999). **Iceland map**: 1 (Tryggvason et al 1983); 2 (Wolfe et al 1997); 3 (Allen et al 1999); 4 (Shen et al 1998); 5 (Ji 1996); 6 (Bijwaard & Spakman 1999); 7 (Helmberger et al 1998); 8 (prediction: Corrieu & Ricard 1999).

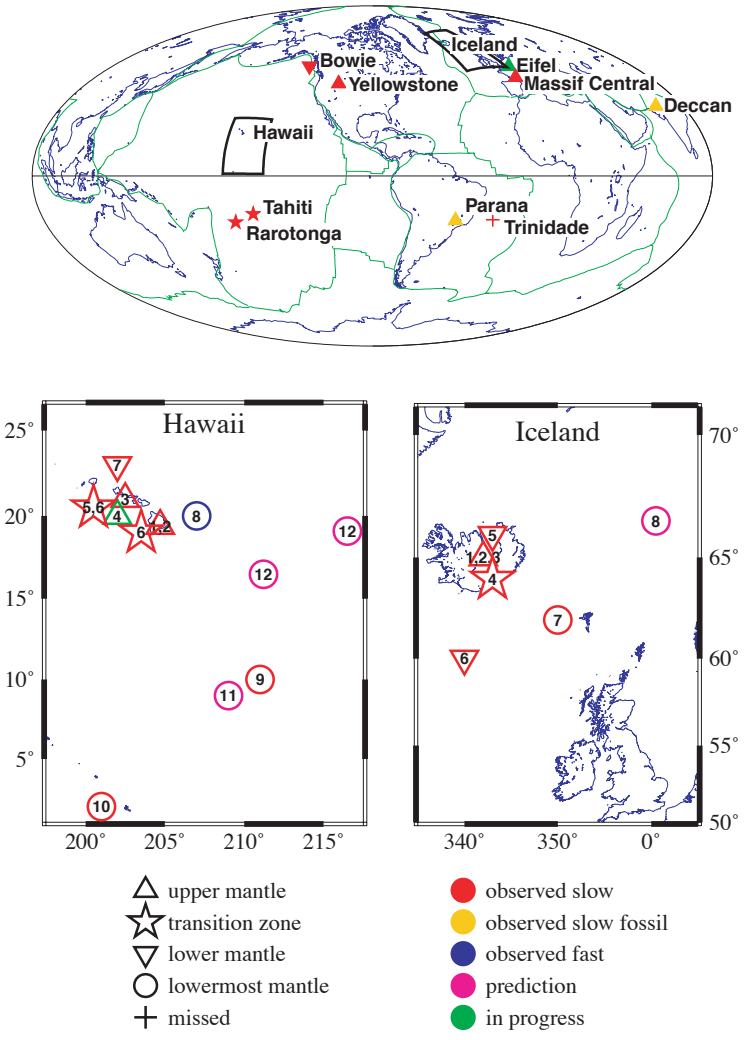

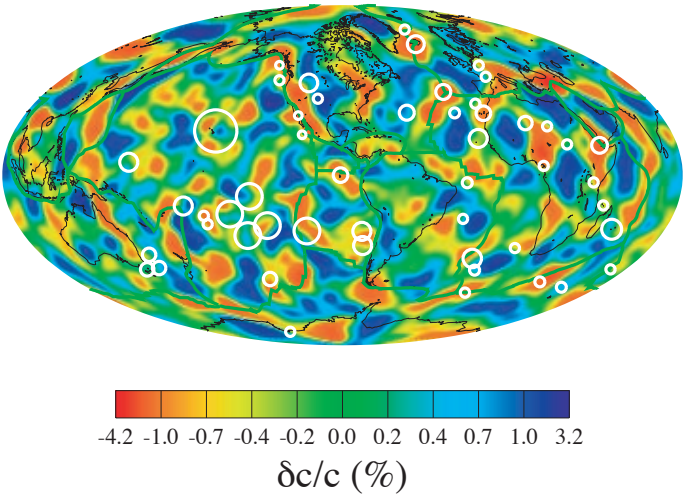

Figure 6 Lateral heterogeneities of the phase velocity c of 75 s-period Rayleigh waves, as derived by Ekström et al (1997). These waves are particularly sensitive to shear-velocity variations just below the lithosphere. Spherical harmonic degrees lower than l = 10 have been removed. Note that several slow patches (warm colors) correspond to hotspot locations (white circles, see Figure 3).

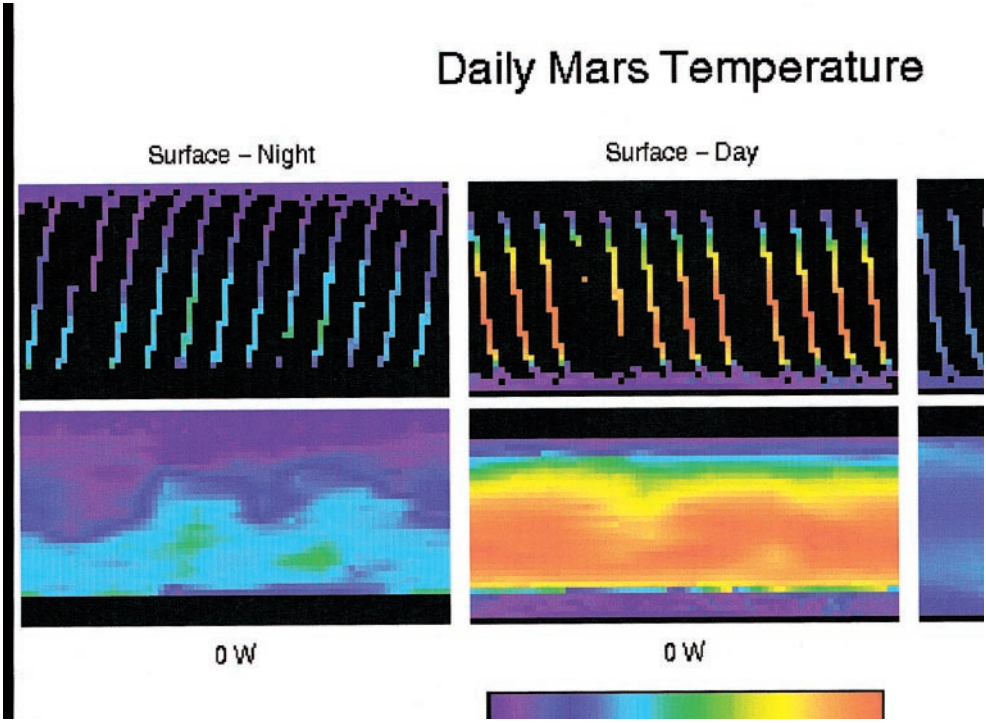

Figure 7 P-wave velocity variations beneath Yellowstone. The image displays a northwest-southeast cross section in the tomographic model of Saltzer & Humphreys (1997). A low-velocity body (in red) extends from the surface to the base of the model at 420 km. The bar at the bottom gives the scale of the variations in percents.

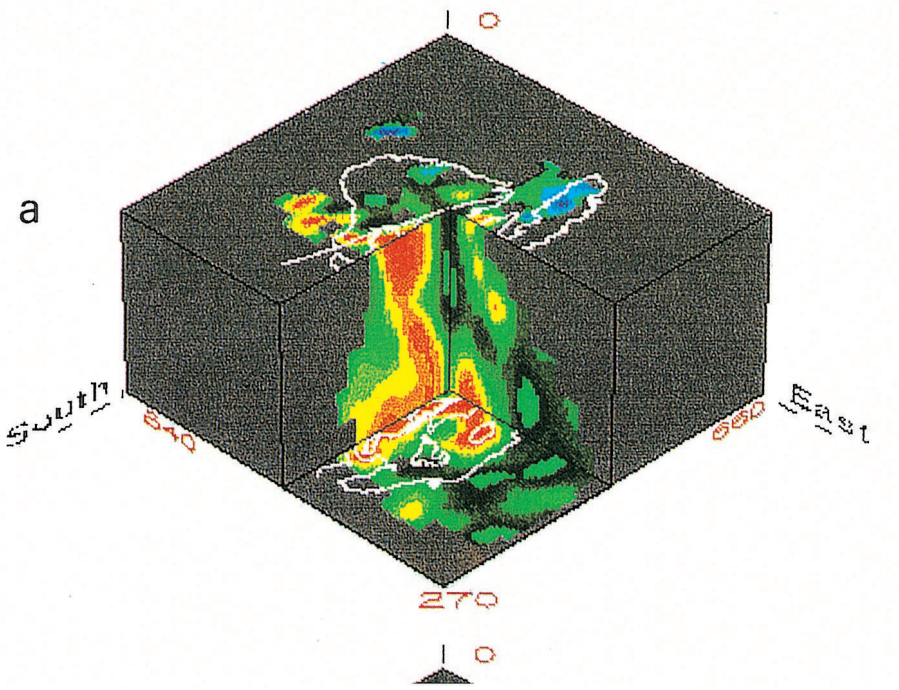

Figure 8 P-wave velocity variations beneath Massif Central (outlined in white at the surface) in France, from Granet et al (1995b). The model extends from the surface down to 660 km depth. The velocity variations range from –2.5% (red) to 2.7% (blue).

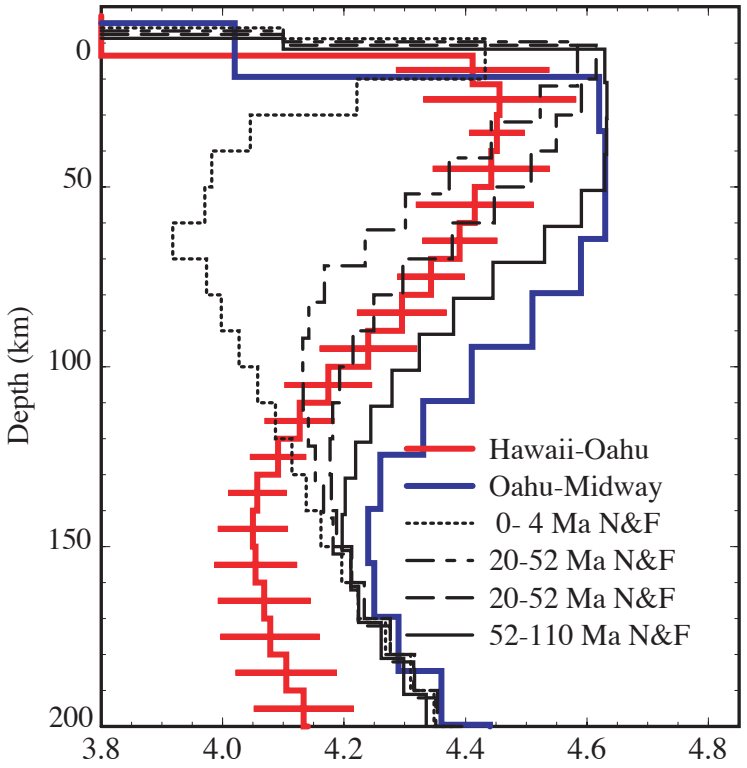

Figure 9 Shear-wave velocity profile on the path from Oahu to Hawaii (see Figure 1) beneath the Hawaiian swell (Tilmann 1999). The profile obtained by Priestley & Tilmann (1999) (*red with error bars*) is compared to normal profiles for various lithospheric ages in the Pacific (Nishimura & Forsyth 1989), and to an earlier profile (*blue*) between Midway and Oahu, derived by Woods & Okal (1996). The profile beneath Hawaii displays shear velocities 5% slower than normal down to at least 200 km.

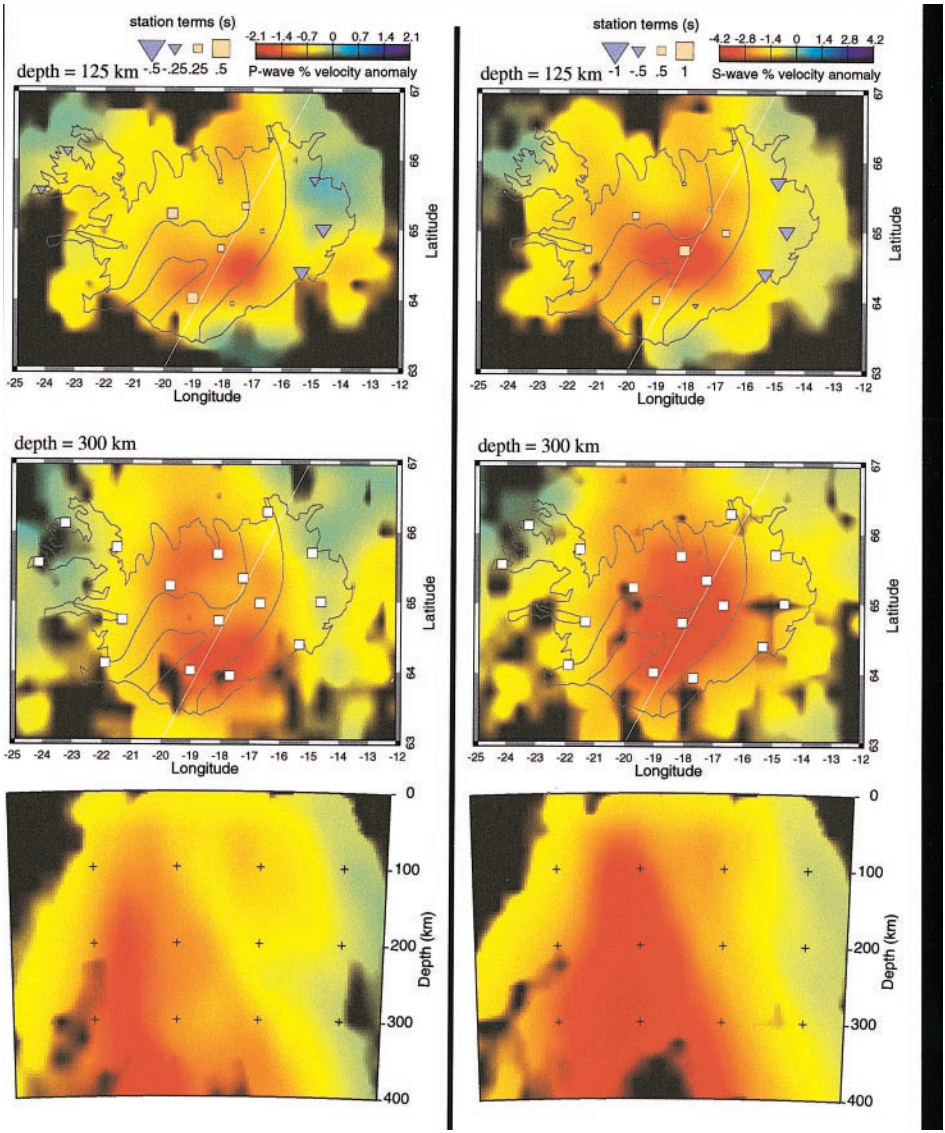

Figure 10 P-wave (left) and S-wave (right) velocity variations beneath Iceland. In each column, the top two panels show horizontal cross sections, at depths of 125 and 300 km. The bottom panel shows the vertical profile along the white line drawn on the map. The scale of the velocity variations is given at the top. From Wolfe et al (1997).

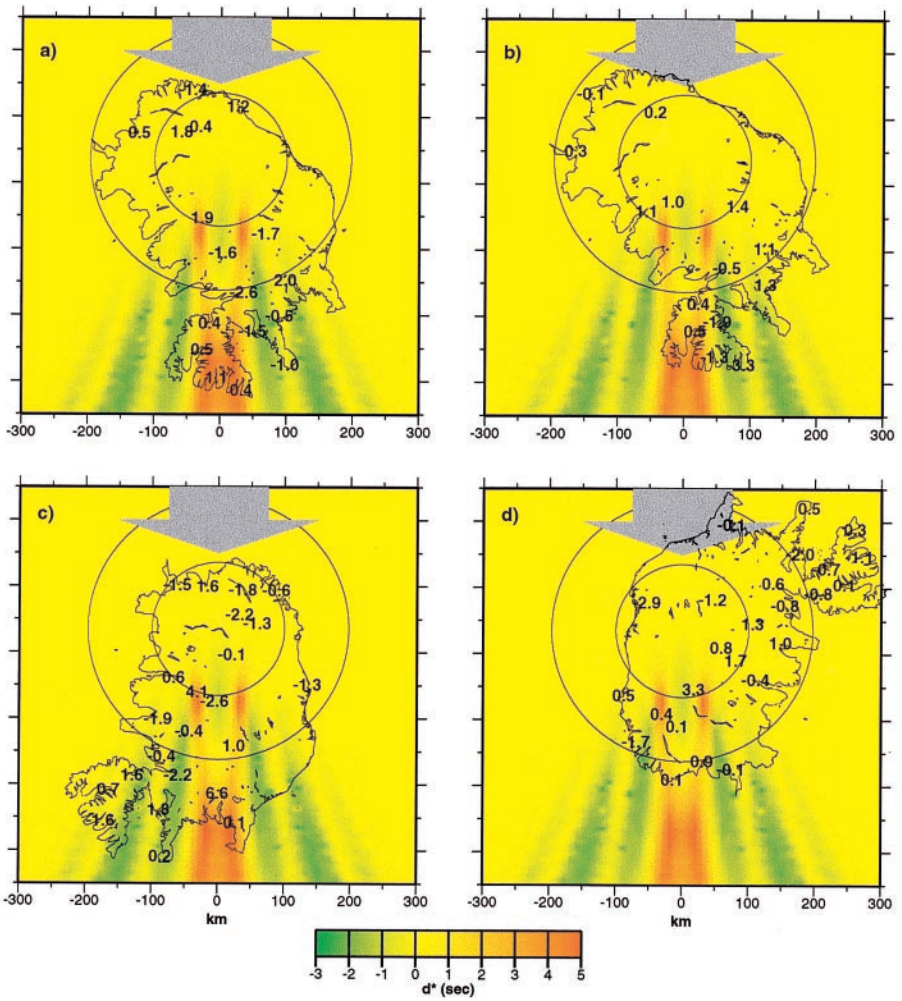

Figure 11 Observed t* variations in Iceland (numbers in seconds) compared to the predictions (*color scale*) for scattering by a plume-like vertical slow anomaly (*circles*). The four plots correspond to rays arriving from different azimuths as indicated by the grey arrow. From Allen et al (1999).

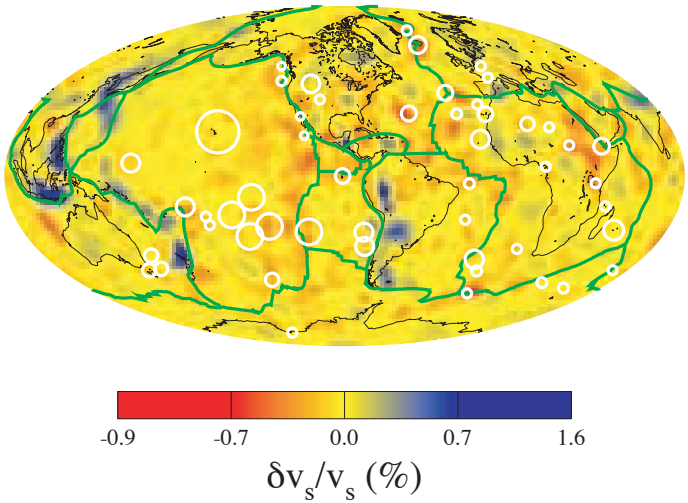

Figure 12 S-wave velocity lateral heterogeneities in a layer between 525 and 650 km. Note the presence of subducting slabs (*blue*) and localized hot regions (*red*). The *white circles* indicate hotspot fluxes, as in Figure 3. From Grand et al (1997).

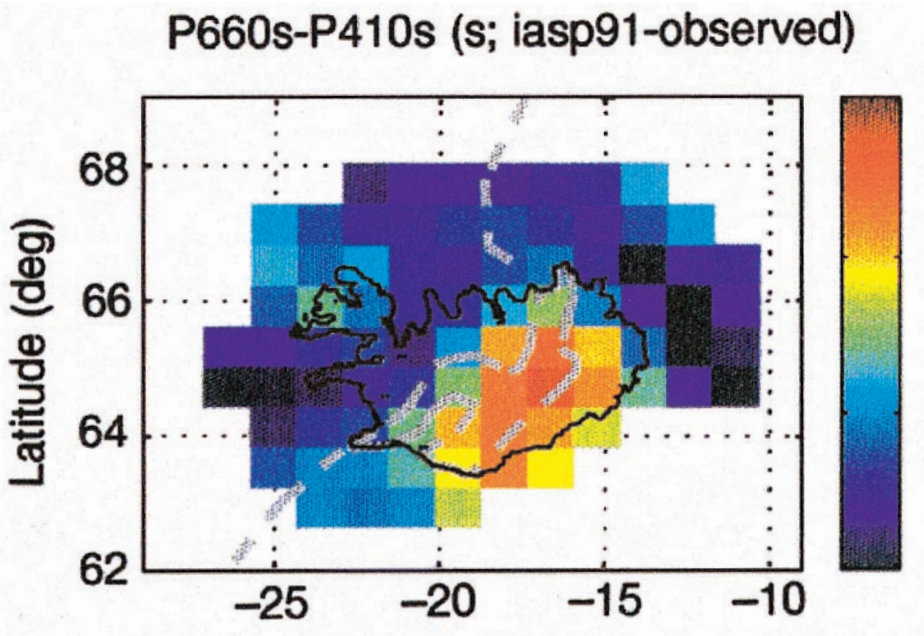

Figure 14 Thickness of the transition zone beneath Iceland, mapped in terms of the time-difference anomaly between $P_{660}s$ and $P_{410}s$ in seconds (scale on the right). Note the thinner-than-normal transition zone beneath southeast Iceland. From Shen et al (1998).

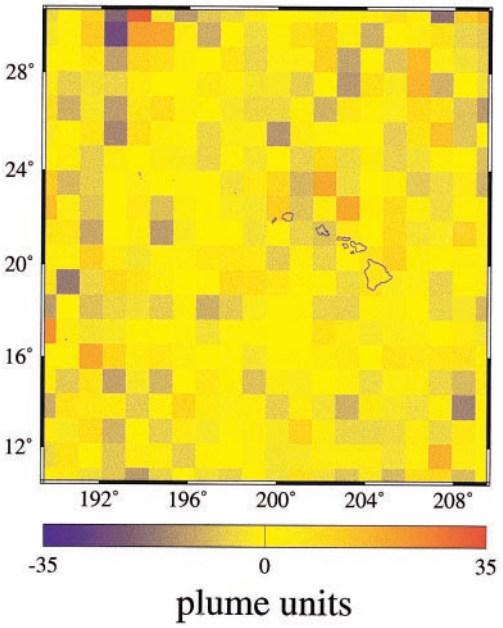

Figure 15 Model of plume-like heterogeneities in the lower mantle that scatter long-period P-waves in the region of Hawaii. The anomalies are expressed in terms of plume-units, which correspond to the effect computed for a standard reference thermal plume. Note the strong scattering slow region (*red*) northwest of Hawaii. From Ji & Nataf 1998b. Also note that the predictions of Corrieu drawn in Ji & Nataf (1998b) have been corrected by Corrieu & Ricard (1999) as drawn in Figure 5.

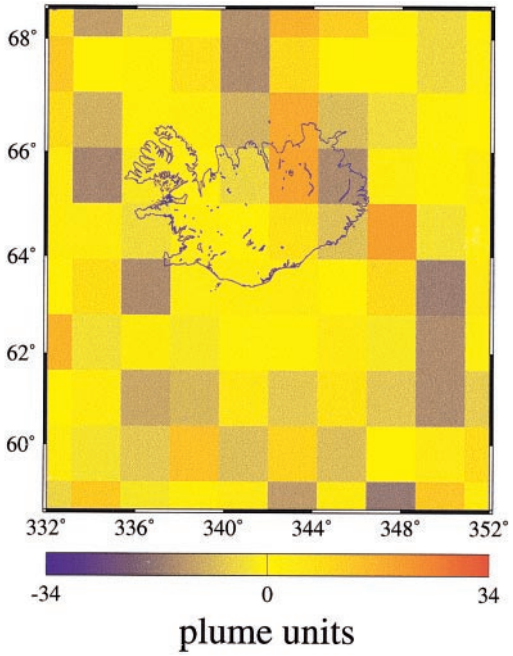

Figure 16 Same as Figure 15 beneath Iceland. Note the strong slow scatterer to the northeast of Iceland. From Ji (1996).

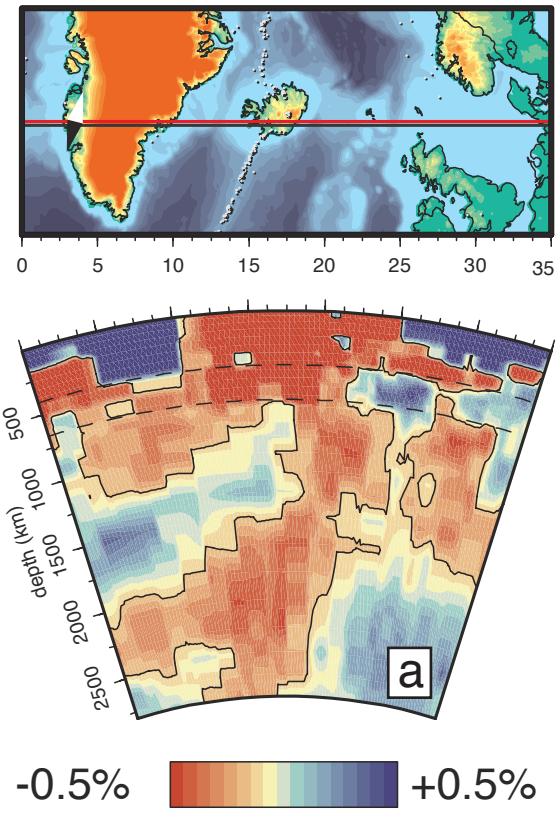

Figure 17 A plume beneath Iceland in the tomographic P-velocity model of Bijwaard et al (1998). From Bijwaard & Spakman (1999).

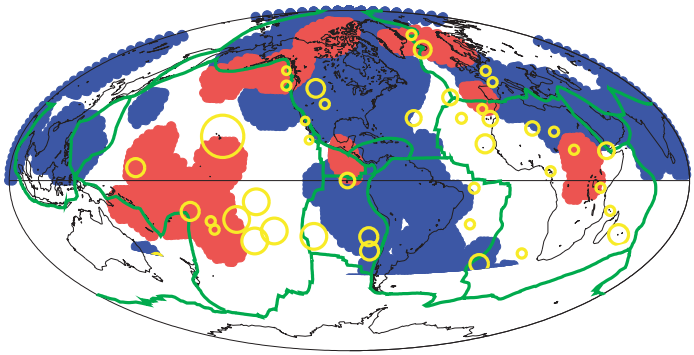

Figure 18 Ultra-Low Velocity Zones (ULVZ) at the base of the mantle. Red zones indicate where ULVZ has been found, whereas it is absent in blue zones. White regions have not been sampled. The yellow circles give the buoyancy fluxes for hotspots, as in Figure 3. Modified fromWilliams et al (1998).

sounded like an impossible task. I hope to have shown in this review that we currently have several observations that confirm the existence of plumes at all depths in the mantle (see summary map in Figure 5). It is probably fair to say that none of the studies I reviewed would appear quite convincing when taken separately; I am nonetheless impressed that, taken together, they all seem to point in the same direction. Today, one may go as far as claiming that plumes do exist, and that some of them rise from the lowermost mantle.

However, almost all the other questions I asked in the introduction still remain unanswered. We know little about how wide and hot plumes are. Most studies report velocity anomalies of about -2% for P-waves and -4% for S-waves, with diameters of around 200 km in the upper mantle—but travel-time tomography is not well suited to give the amplitudes of seismic velocity anomalies in plumes. The few efforts to use the amplitude of scattered waves to better constrain the velocity anomalies yielded values that range from large (12% for S-waves in Allen et al 1999) to huge (30% or more in Ji & Nataf 1998b). If these values were confirmed, they would clearly imply more than just a temperature effect.

In turn, this could make it difficult to directly infer the excess temperature in plumes from observed velocity anomalies, even though this would be very useful from a dynamical point of view. Indeed, there seems to be a contradiction between the large temperature contrast ($\Delta T \simeq 1{,}000$ K) estimated across the lower thermal boundary layer at the base of the mantle and the excess temperature calculated for the source of plumes by downward extrapolation of their upper mantle values (Albers & Christensen 1996, Farnetani 1997). The Hawaiian plume, with its very large buoyancy flux, should not lose much of its temperature excess on its way up to the surface; therefore, if the temperature excess is only 250 K near the surface, it should be no more than 500 K at the source of this plume (Albers & Christensen 1996). If its source lies at the core-mantle boundary, as recent results suggest (Ji & Nataf 1998b, Russell et al 1998), it is difficult to reconcile the observed volcanism of Hawaii with a temperature drop of 1,000 K above the core-mantle boundary. One way out is to invoke the existence of a chemically distinct and denser layer at the base of the mantle, which absorbs part of the temperature drop (Albers & Christensen 1996). The effect on plumes was examined by Farnetani (1997), who found that a layer 30 km thick and 5% denser could do the job. This situation was further documented by Davaille (1999a,b), who performed laboratory convection experiments on layered systems. She found that several different phenomena can take place, with small-scale interaction yielding plume-like structures, whereas large-scale domes can be created by a large uplift on the interface between the two layers. Deciphering the fine structure of the lowermost mantle beneath Hawaii and the south Pacific should prove most useful in this respect.

Another important question remains unanswered: Are there different kinds of plumes and do they all rise from the same depth? The large range of buoyancy fluxes of hotspots is difficult to account for if they all start with the same excess

temperature (Albers & Christensen 1996). Indeed, plumes as weak as Bowie should lose much of their temperature excess before reaching the surface, where they would not be hot enough to produce melt (Albers & Christensen 1996). In fact, weak plumes should be swept away by the ''mantle wind'' (Steinberger & O'Connell 1998, Corrieu & Ricard 1999)—hence the idea that some plumes come from a more shallow thermal boundary layer. The geochemical evidence also points toward there being several different kinds of plumes (Hofmann 1997). This is another challenge for seismologists; so far, very few hotspots have received their attention (see Figure 5), with most studies focusing on Hawaii and Iceland. However, there is one report of a lower-mantle signature for the Bowie hotspot (Nataf & VanDecar 1993). If confirmed, this would have strong implications for understanding the dynamics of mantle plumes. High-resolution travel-time tomography now permits researchers to address some of these issues (Goes et al 1999).

Finally, much needs to be done to improve our understanding of how plume material interacts with the lithosphere. This is a field that involves many different disciplines, and in which seismology should play an increasing role.

Under mature oceanic plates, plumes seem to produce well-defined swells, but only limited seismological information is available. Near-field surface wave investigations reveal a thick, low-velocity layer beneath the lithosphere between Oahu and Hawaii (Priestley & Tilmann 1999).

Near oceanic ridges, there is good geochemical evidence that plume material flows up along the base of the lithosphere toward the ridge, for distances as large as 1,000 km (Schilling 1991). No seismic evidence exists yet to document this behavior.

Beneath the continents, the situation is even more complex. Ebinger & Sleep (1998) proposed that a single plume beneath East Africa could feed all the African hotspots (Afar, Hoggar, Tibesti, etc) as plume material spreads beneath the thick and ragged continental lithosphere. When it finds its way up in lithospheric holes, plume material rises, decompresses, and melts. This again presents a challenge for seismologists trying to document such a fascinating behavior. Regional travel-time tomography models beneath continental hotspots show no evidence for plume material spreading horizontally beneath the lithosphere (Granet et al 1995b, Saltzer & Humphreys 1997). Saltzer & Humphreys mention this lack of evidence for Yellowstone, which leads them to question the plume model. However, one should bear in mind that this type of seismic investigation is quite insensitive to features with a large lateral extent. If valid, the observation of Saltzer & Humphreys could indicate that plume material flows in a complex manner beneath the Yellowstone area.

Finally, the discovery of fossil plumes that mark where plume material first pierced the lithosphere brings an unexpected twist to the question of plume-lithosphere interaction (VanDecar et al 1995, Kennett & Widiyantoro 1999).

Seismologists are now fully aware of the geodynamical importance of hotspots. Today we have good seismic evidence for mantle plumes, but many ques-

tions still remain unanswered. If seismological investigations of mantle plumes carry on at the same pace as they have during these past few years, though, I have no doubt that these questions will be replaced by new, unexpected ones—which is the real sign of scientific progress.

Visit the Annual Reviews home page at www.AnnualReviews.org.

LITERATURE CITED

Albers M, Christensen UR. 1996. The excess temperature of plumes rising from the core-mantle boundary. *Geophys. Res. Lett.* 23:3567–70

Allen RM, Nolet G, Morgan WJ, Vogfjörd K, Bergsson BH, et al. 1999. The thin hot plume beneath Iceland. *Geophys. J. Int.* 137:51–63

Anderson DL. 1995. Lithosphere, asthenosphere, and perisphere. *Rev. Geophys.* 33:125–49

Anderson DL. 1998. The scales of mantle convection. *Tectonophysics* 284:1–17

Anderson DL, Tanimoto T, Zhang YS. 1992. Plate tectonics and hotspots: the third dimension. *Science* 256:1645–50

Bijwaard H, Spakman W. 1999. Tomographic evidence for a narrow whole mantle plume below Iceland. *Earth Planet. Sci. Lett.* 166:121–26

Bijwaard H, Spakman W, Engdahl ER. 1998. Closing the gap between regional and global travel time tomography. *J. Geophys. Res.* 103:30055–78

Bjarnason IT, Wolfe C, Solomon SC, Gudmundson G. 1996a. Initial results from the ICEMELT experiment: body-wave delay times and shear-wave splitting across Iceland. *Geophys. Res. Lett.* 23:459–62

Bjarnason IT, Wolfe C, Solomon SC. Gudmundson G. 1996b. Correction. *Geophys. Res. Lett.* 23:903

Boehler R. 1993. Temperatures in the Earth's core from melting point measurements of iron at high static pressures. *Nature* 363:534–36

Bréger L, Romanowicz B. 1998. Three-dimensional structure at the base of the mantle beneath the central Pacific. *Science* 282:718–20

Campbell IH, Griffiths RW. 1990. Implications of mantle plume structure for the evolution of flood basalts. *Earth Planet. Sci. Lett.* 99:79–93

Capdeville Y, Stutzmann E, Montagner JP. 2000. Effect of a plume on long period surface waves computed with normal mode coupling. *Phys. Earth Planet. Inter.* In press

Corrieu V, Ricard Y. 1999. Hotspots and mantle dynamics. Accepted in *Geophys. J. Int.*

Dahlen FA, Hung SH, Nolet G. 2000. Fréchet kernels for finite-frequency traveltimes—I. Theory. *Geophys. J. Int.* In press

Davaille A. 1999a. Simultaneous generation of hotspots and superswells by convection in a heterogeneous planetary mantle. *Nature* 402:756–60

Davaille A. 1999b. Two-layer thermal convection in miscible viscous fluids. *J. Fluid Mech.* 379:223–53

Davies GF. 1988. Ocean bathymetry and mantle convection: 1. Large-scale flow and hotspots. *J. Geophys. Res.* 93:10467–80

Devaney AJ. 1984. Geophysical diffraction tomography. *IEEE Trans. Geosci. Remote Sensing* 22:3–13

Duncan RA, Richards MA. 1991. Hotspots, mantle plumes, flood basalts and true polar wander. *Rev. Geophys.* 29:31–50

Dziewonski AM. 1984. Mapping the lower mantle. *J. Geophys. Res.* 89:5929–52

Ebinger CJ, Sleep NH. 1998. Cenozoic magmatism throughout east Africa resulting from impact of a single plume. *Nature* 395:788–91

Ekström G, Tromp J, Larson EWF. 1997. Measurements and global models of surface wave propagation. *J. Geophys. Res.* 102:8137–57

Ellsworth WL. 1977. PhD thesis. Massachusetts Institute of Technology.

Ellsworth WL, Koyanagi RY. 1977. Three-dimensional crust and mantle structure of Kilauea volcano, Hawaii. *J. Geophys. Res.* 82:5379–94

Emery V, Maupin V, Nataf HC. 1999. Scattering of S waves diffracted at the core-mantle boundary: forward modelling. *Geophys. J. Int.* 139:325–44

Evans JR. 1982. Compressional wave velocity structure of the upper 350 km under the eastern Snake River Plain near Rexburg, Idaho. *J. Geophys. Res.* 87:2654–70

Farnetani CG. 1997. Excess temperature of mantle plumes: the role of chemical stratification across D″. *Geophys. Res. Lett.* 24:1583–86

Froidevaux C, Brousse R, Bellon H. 1974. Hot spot in France? *Nature* 248:749–51

Garnero EJ. 2000. Heterogeneity of the lowermost mantle. *Annu. Rev. Earth Planet. Sci.* 28:509–37

Garnero EJ, Helmberger DV. 1995. A very slow basal layer underlying large-scale low-velocity anomalies in the lower mantle beneath the Pacific: evidence from core phases. *Phys. Earth Planet. Inter.* 91:161–76

Garnero EJ, Revenaugh JS, Williams Q, Lay T, Kellogg LH. 1998. Ultralow velocity zone at the core-mantle boundary. In *The Core-Mantle Boundary,* ed. M Gurnis, ME Wysession, E Knittle, BA Buffett, pp. 319–34. Washington, DC: AGU

Goes S, Spakman W, Bijwaard H. 1999. A lower mantle source for central European volcanism. *Science* 286:1928–31

Grand SP. 1994. Mantle shear structure beneath the Americas and surrounding oceans. *J. Geophys. Res.* 99:11591–621

Grand SP, van der Hilst RD, Widiyantoro S. 1997. Global seismic tomography: a snapshot of convection in the Earth. *GSA Today* 7:1–7

Granet M, Stoll G, Dorel J, Achauer U, Poupinet, Fuchs K. 1995a. Massif Central (France): new constraints on the geodynamical evolution from teleseismic tomography. *Geophys. J. Int.* 121:33–48

Granet M, Wilson M, Achauer U. 1995b. Imaging a mantle plume beneath the French Massif Central. *Earth Planet. Sci. Lett.* 136:281–96

Griffiths RE, Campbell IH. 1990. Stirring and structure in mantle starting plumes. *Earth Planet. Sci. Lett.* 99:66–78

Griot DA, Montagner JP, Tapponnier P. 1998. Phase velocity structure from Rayleigh and Love waves in Tibet and its neighbouring regions. *J. Geophys. Res.* 103:21215–32

Gudmundsson O. 1996. On the effect of diffraction on traveltime measurements. *Geophys. J. Int.* 124:304–14

Hadiouche O, Jobert N, Montagner JP. 1989. Anisotropy of the African continent inferred from surface waves. *Phys. Earth Planet. Inter.* 58:61–81

Helffrich G, Sacks S. 1992. Are plumes visible to seismic waves? *EOS (Trans. AGU)* 73(suppl.):403

Helmberger DV, Wen L, Ding X. 1998. Seismic evidence that the source of the Iceland hotspot lies at the core-mantle boundary. *Nature* 396:251–55

Hofmann AW. 1997. Mantle geochemistry: the message from oceanic volcanism. *Nature* 385:219–29

Hung SH, Dahlen FA, Nolet G. 2000. Fréchet kernels for finite-frequency traveltimes—II. Examples. *Geophys. J. Int.* In press

Iyer HM, Evans JR, Zandt G, Stewart RM, Coakley JM, Roloff JN. 1981. A deep low-velocity body under the Yellowstone caldera, Wyoming: delineation using P-wave residuals and tectonic interpretation: summary. *Geol. Soc. Am. Bull.* 92:792–98

Ji Y. 1996. *Tomographie par diffraction et détection de panaches mantelliques dans le manteau inférieur.* Thèse. Univ. Paris 7. 108 pp.

Ji Y, Nataf HC. 1998a. Detection of mantle plumes in the lower mantle by diffraction tomography: theory. *Earth Planet. Sci. Lett.* 159:87–98

Ji Y, Nataf HC. 1998b. Detection of mantle plumes in the lower mantle by diffraction tomography: Hawaii. *Earth Planet. Sci. Lett.* 159:99–115

Jordan TH. 1975. The continental tectosphere. *Rev. Geophys.* 13:1–12

Kanasewich ER, Ellis RM, Chapman CH, Gutowski PR. 1972. Teleseismic array evidence for inhomogeneities in the lower mantle and the origin of the Hawaiian islands. *Nature* 239:99

Kanasewich ER, Ellis RM, Chapman CH, Gutowski PR. 1973. Seismic array evidence of a core boundary source for the Hawaiian linear volcanic chain. *J. Geophys. Res.* 78:1361–71

Kanasewich ER, Ellis RM, Chapman CH, Gutowski PR. 1975. Reply. *J. Geophys. Res.* 80:1920–22

Kanasewich ER, Gutowski PR. 1975. Detailed seismic analysis of a lateral mantle inhomogeneity. *Earth Planet. Sci. Lett.* 25:379–84

Katzman R, Zhao L, Jordan T. 1998. High-resolution, two-dimensional vertical tomography of the central Pacific using ScS reverberations and frequency-dependent travel times. *J. Geophys. Res.* 103:17933–71

Kennett BLN, Widiyantoro S. 1999. A low seismic wavespeed anomaly beneath northwestern India: a seismic signature of the Deccan plume? *Earth Planet. Sci. Lett.* 165:145–55

Kind R, Vinnik LP. 1988. The upper-mantle discontinuities underneath the GRF array from P-to-S converted phases. *J. Geophys.* 62:138–47

Kulakov IYu, Tychkov SA, Keselman SI. 1995. Three-dimensional structure of lateral heterogeneities in P-velocities in the upper mantle of the southern margin of Siberia and its preliminary geodynamic interpretation. *Tectonophysics* 241:239–57

Lambeck K, Johnston P, Smither C, Nakada M. 1996. Glacial rebound of the British Isles—III. Constraints on mantle viscosity. *Geophys. J. Int.* 125:340–54

Laske G, Phipps Morgan J, Orcutt JA. 1999. First results from the Hawaiian SWELL pilot experiment. *Geophys. Res. Lett.* 26:3397–400

Lay T, Helmberger DV. 1983. A lower mantle S wave triplication and the shear velocity structure of D″. *Geophys. J. R. Astron. Soc.* 75:799–837

Lay T, Young CJ. 1996. Imaging scattering structures in the lower mantle by migration of long-period S waves. *J. Geophys. Res.* 101:20023–40

Li X, Kind R, Priestley K, Sobolev SV, Tilmann F, Yuan X, Weber M. 1999. Mapping the Hawaii plume conduit with receiver functions. Submitted to *Nature*

Lognonné P, Romanowicz B. 1990. Modelling of coupled normal modes of the Earth: the spectral method. *Geophys. J. Int.* 102:365–95

Matte P, Mattauer M, Olivet JM, Griot DA. 1997. Continental subductions beneath Tibet and the Himalayan orogeny: a review. *Terra Nova* 9:264–70

Maupin V. 1992. Modelling of laterally trapped surface waves with application to Rayleigh waves in the Hawaiian swell. *Geophys. J. Int.* 110:553–70

McKenzie DP. 1984. The generation and compaction of partial molten rocks. *J. Petrol.* 25:713–65

McNutt M, Fischer K. 1987. The South Pacific superswell. In *Seamounts, Islands and Atolls,* Geophys. Monogr. Ser., Vol. 43, ed. B Keating, R Batiza, pp. 25–34. Washington, DC: AGU

Montagner JP. 1994. Can seismology tell us anything about convection in the mantle? *Rev. Geophys.* 32:115–37

Morgan WJ. 1971. Convective plumes in the lower mantle. *Nature* 230:42–43

Morgan WJ. 1972. Plate motions and deep mantle convection. *Mem. Geol. Soc. Am.* 132:7–22

Nataf HC, Houard S. 1993. Seismic discontinuity at the top of D″: a world-wide feature? *Geophys. Res. Lett.* 20:2371–74

Nataf HC, Lay T, Anderson DL, Okal EA. 1981. Reassessment of a reported S-delay under Trinidade. *Geophys. Res. Lett.* 8:1027–30

Nataf HC, Ricard Y. 1996. 3SMAC: an a priori tomographic model of the upper mantle based on geophysical modeling. *Phys. Earth Planet. Inter.* 95:101–22

Nataf HC, VanDecar J. 1993. Seismological detection of a mantle plume? *Nature* 364:115–20

Neele F, Lognonné P, Romanowicz B, Snieder R. 1989. Effect of sharp lateral heterogeneity on the Earth's normal modes. *Geophys. Res. Lett.* 16:397–400

Neele F, Snieder R. 1991. Topography of the 400 km discontinuity from observations of long-period P400P phases. *Geophys. J. Int.* 109:670–82

Nishimura C, Forsyth D. 1989. The anisotropic structure of the upper mantle in the Pacific. *Geophys. J. Int.* 96:203–29

Okal EA, Anderson DL. 1975. A study of lateral heterogeneities in the upper mantle by multiple ScS travel-time residuals. *Geophys. Res. Lett.* 2:313–16

Olson P, Singer HA. 1985. Creeping plumes. *J. Fluid Mech.* 158:511–31

Paulssen H. 1988. Evidence for a sharp 670-km discontinuity as inferred from P-to-S converted waves. *J. Geophys. Res.* 93:10489–500

Priestley K, Tilmann F. 1999. Shear-wave structure of the lithosphere above the Hawaiian hot spot from two-station Rayleigh wave phase velocity measurements. *Geophys. Res. Lett.* 26:1493–96

Raikes S, Bonjer KP. 1983. Large-scale mantle heterogeneity beneath the Rhenish Massif and its vicinity from teleseismic P-residuals measurements. In *Plateau Uplift: The Rhenish Shield—A Case History,* ed. K Fuchs et al, pp. 315–31. Berlin: Springer-Verlag. 411 pp.

Revenaugh J. 1995. A scattered-wave image of subduction beneath the transverse ranges. *Science* 268:1888–92

Ribe N, Christensen UR. 1994. Melt generation by plumes: a study of Hawaiian volcanism. *J. Geophys. Res.* 99:669–82

Ribe NM, de Valpine DP. 1994. The global hotspot distribution and instability in D″. *Geophys. Res. Lett.* 21:1507–10

Ricard Y, Vigny C, Froidevaux C. 1989. Mantle heterogeneities, geoid and plate motions: a Monte-Carlo inversion. *J. Geophys. Res.* 94:13739–54

Richards MA, Griffiths RW. 1988. Deflection of plumes by mantle shear flow: experimental results and a simple theory. *Geophys. J. Int.* 94:367–76

Richards MA, Hager BH. 1984. Geoid anomalies in a dynamic Earth. *J. Geophys. Res.* 89:5987–6002

Ritter JRR, Christensen UR, Achauer U, Bahr K, Weber MH. 1998. Search for a mantle plume under central Europe. *EOS Am. Union Trans.* 79:420

Ritter JRR, EIFEL working group. 1997. Investigation of the seismic structure below the lower Rhine Graben and the Eifel volcanic fields. *Proc. IGCP 400 Meeting, Dublin, Communications of the Dublin Institute for Advanced Studies, Series D Geophysical Bulletin* 48:117–19

Roult G, Rouland D, Montagner JP. 1994. Antarctica II: Upper-mantle structure from velocities and anisotropy. *Phys. Earth Planet. Inter.* 84:33–57

Russell SA, Lay T, Garnero EJ. 1998. Seismic evidence for small-scale dynamics in the lowermost mantle at the root of the Hawaiian hotspot. *Nature* 396:255–58

Saltzer RL, Humphreys ED. 1997. Upper mantle P wave velocity structure of the eastern Snake River Plain and its relationship to geodynamic models of the region. *J. Geophys. Res.* 102:11829–41

Schilling JG. 1991. Fluxes and excess temperatures of mantle plumes inferred from their interaction with migrating mid-ocean ridges. *Nature* 352:397–403

Shen Y, Solomon SC, Bjarnason IT, Wolfe CJ. 1998. Seismic evidence for a lower-mantle origin of the Iceland plume. *Nature* 395:62–65

Sidorin I, Gurnis M, Helmberger DV. 2000. Dynamics of a phase change at the base of the mantle consistent with seismological observations. *J. Geophys. Res*. In press

Sleep NH. 1990. Hotspots and mantle plumes: some phenomenology. *J. Geophys. Res*. 95:6715–36

Sparrow EM, Husar RB, Goldstein RJ. 1970. Observations and other characteristics of thermals. *J. Fluid Mech*. 41:793–800

Steinberger BM, O'Connell RJ. 1998. Advection of plumes in mantle flow; implications on hotspot motion, mantle viscosity and plume distribution. *Geophys. J. Int*. 132:412–34

Tilmann FJ, McKenzie D, Priestley KF. 1998. P and S wave scattering from mantle plumes. *J. Geophys. Res*. 103:21145–63

Tilmann JT. 1999. *The seismic structure of the upper mantle beneath Hawaii*. PhD thesis. Univ. Cambridge. 177 pp.

Tryggvason K, Husebye ES, Stefánsson R. 1983. Seismic image of the hypothesized Icelandic hot spot. *Tectonophysics* 100:97–118

Turner DL, Jarrard RD, Forbes RB. 1980. Geochronology and origin of the Pratt-Welker seamount chain, Gulf of Alaska: a new pole of rotation for the Pacific plate. *J. Geophys. Res*. 85:6547–56

VanDecar JC, James DE, Assumpçao M. 1995. Seismic evidence for a fossil mantle plume beneath South America and implications for plate driving forces. *Nature* 378:25–31

van der Hilst RD, Widiyantoro S, Engdahl ER. 1997. Evidence for deep mantle circulation from global tomography. *Nature* 386:578–84

Vinnik LP. 1977. Detection of waves converted from P to SV in the mantle. *Phys. Earth Planet. Inter.* 15:39–45

Vinnik LP, Chevrot S, Montagner JP. 1997. Evidence for a stagnant plume in the transition zone? *Geophys. Res. Lett*. 24:1007–10

Watson S, McKenzie DP. 1991. Melt generation by plumes: a study of Hawaiian mechanism. *J. Petrol*. 32:501–37

Weidner DJ, Wang Y. 1998. Chemical- and Clapeyron-induced buoyancy at the 660 km discontinuity. *J. Geophys. Res*. 103:7431–41

Weinstein SA, Olson P. 1989. The proximity of hotspots to convergent and divergent plate boundaries. *Geophys. Res. Lett*. 16:433–436

Wessel P, Smith WHF. 1991. Free software helps map and display data. *EOS Trans. AGU* 72:441

Whitehead JA, Luther DS. 1975. Dynamics of laboratory diapir and plume models. *J. Geophys. Res*. 80:705–17

Wielandt E. 1987. On the validity of the ray approximation for interpreting delay times, In *Seismic Tomography,* ed. G Nolet, pp. 85–98. Dordrecht, The Netherlands: Reidel

Williams Q, Garnero EJ. 1996. Seismic evidence for partial melt at the base of Earth's mantle. *Science* 273:1528–30

Williams Q, Revenaugh JS, Garnero EJ. 1998. A correlation between ultra-low basal velocities in the mantle and hotspots. *Science* 281:546–49

Wilson JT. 1963. A possible origin of the Hawaiian island. *Can. J. Phys*. 41:863–68

Wittlinger G, Masson F, Poupinet G, Tapponnier P, Jiang M, et al. 1996. Seismic tomography of northern Tibet and Kunlun: evidence for crustal blocks and mantle velocity contrasts. *Earth Planet. Sci. Lett*. 139:263–80

Wolfe CJ, Bjarnason IT, VanDecar JC, Solomon SC. 1997. Seismic structure of the Iceland mantle plume. *Nature* 385:245–47

Woods M, Lévêque JJ, Okal E, Cara M. 1991. Two-station measurements of Rayleigh wave group velocity along the Hawaiian swell. *Geophys. Res. Lett*. 18:105–8

Woods M, Okal E. 1996. Rayleigh-wave dispersion along the Hawaiian swell: a test of lithospheric thinning by thermal rejuvenation at a hot spot. *Geophys. J. Int.* 125:325–39

Wright C. 1975. Comments on ''Seismic array evidence of a core boundary source for the Hawaiian linear volcanic chain'' by E. R. Kanasewich et al. *J. Geophys. Res.* 80:1915–19

Zerr A, Diegeler A, Boehler R. 1998. Solidus of Earth's deep mantle. *Science* 281:243–46

Zhang YS, Tanimoto T. 1993. High resolution global upper mantle structure and plate tectonics. *J. Geophys. Res.* 98:9793–823

Zhao L, Jordan TH. 1998. Sensitivity of frequency-dependent traveltimes to laterally heterogeneous, anisotropic Earth structure. *Geophys. J. Int.* 133:683–704

Annual Review of Earth and Planetary Science
Volume 28, 2000

CONTENTS